

**Effect of Compliant Boundaries on  
Weakly Nonlinear Shear Waves in Channel Flow**

Thesis by

James Michael Rotenberry

In Partial Fulfillment of the Requirements

for the Degree of

Doctor of Philosophy

California Institute of Technology

Pasadena, California

June, 1989

(Submitted 12 August 1988)

# Acknowledgment

I would like to thank Professor Philip G. Saffman for his guidance of my investigations. His mathematical and physical understanding yielded critical insights into the most difficult aspects of this work. I gratefully acknowledge the outstanding facilities he put at my disposal.

I wish to express my appreciation for the Charles Lee Powell Fellowship I received in the academic year 1986-87 and for the Caltech Graduate Research Assistantships funded by ONR Contract # N00014-85-K-0205 and ARO Contract # DAAG29-85-K-0092.

The computations for my investigations were carried out primarily on the Caltech Applied Mathematics Sun network. Additional computations were performed on the San Diego Supercomputing Center's Cray X-MP/48.

I would like to thank Michael Ward, James Kamm, and Saleh Tanveer for their helpful comments concerning this work, and I have also benefited from discussions with M. Landman, D.S. Cohen, T. Minzoni, P.J. Blennerhassett, I. Soibelman, and E. Doedel. I would also like to thank Jeanette Butler for many helpful conversations.

Finally, I would like to thank my wife, Sara, and son, Alex, for their support, encouragement, understanding, and sacrifice during my years as a graduate student.

# Abstract

There exists a critical Reynolds number (at which a linear instability first appears) for an incompressible fluid flowing in a channel with compliant walls (Hains and Price, [1962]). It is proven that, for fixed non-dimensionalized wall parameters, to any unstable disturbance in three dimensions there corresponds an unstable disturbance in two dimensions at a lower Reynolds number. Consequently, the Ginzburg-Landau equation is used to study the weakly nonlinear two-dimensional evolution of a disturbance in a channel with compliant walls for Reynolds number near its critical value. The coefficients of this equation are found by numerically integrating solutions of the Orr-Sommerfeld equation and its adjoint as well as solutions of the perturbation equations.

For rigid walls the finite amplitude two-dimensional plane wave solution that bifurcates from laminar Poiseuille flow at the critical Reynolds number is itself unstable to two-dimensional disturbances. It is found that for compliant walls this solution is stable to disturbances of the same type.

The formalism developed by Landman [1987] is used to study a class of quasisteady solutions to the Ginzburg-Landau equation. This class includes solutions describing a transition from the laminar solution to finite amplitude states and non-periodic, “chaotic” attracting sets. It is shown that for compliant walls the transition solutions persist while the “chaotic” ones do not.

# Preface

A person familiar with scientific literature will immediately notice that I have ignored the usual convention of using the word “we” when I really mean “I”. This choice is deliberate. One reason I made this choice is that any mistakes, errors, or omissions in this work are my responsibility, not ours, and I do not wish to share this responsibility, even by implication. Another reason is the use of “we” in a work by a single author sounds too aristocratic and presumptuous, especially for a U.S. citizen and a native of the state of Texas.

The text, I find, is much more readable.

# Contents

|  |            |
|--|------------|
| <b>Acknowledgment</b>                                    | <b>ii</b>  |
| <b>Abstract</b>  | <b>iii</b> |
| <b>Preface</b>   | <b>iv</b>  |
| <b>List of Figures</b>                                   | <b>vii</b> |
| <b>List of Tables</b>                                    | <b>ix</b>  |
| <b>1 Introduction</b>                                    | <b>1</b>   |
| <b>2 Squire's Theorem</b>                                | <b>8</b>   |
| <b>3 Ginzburg-Landau equation</b>                        | <b>12</b>  |
| 3.1 Derivation of the Ginzburg-Landau equation . . . . . | 12         |
| 3.2 The Compliant Boundary Conditions . . . . .          | 18         |
| 3.3 Numerical Results . . . . .                          | 28         |
| <b>4 Quasisteady solutions</b>                           | <b>34</b>  |
| <b>5 Conclusions</b>                                     | <b>47</b>  |
| <b>A Orr-Sommerfeld maximum growth rate</b>              | <b>50</b>  |

|  |           |
|--|-----------|
| <b>B The calculation of <math>c_g</math></b> | <b>53</b> |
| <b>Bibliography</b>                          | <b>55</b> |

# List of Figures

|     |  |    |
|-----|--|----|
| 1.1 | The definition of $\eta$ and $\xi$ . . . . .   | 2  |
| 1.2 | The curve of marginal stability. . . . .   | 4  |
| 3.1 | The displacement of the upper and lower walls. . . . .   | 19 |
| 3.2 | Configuration space for two-dimensional finite amplitude waves in Poiseuille flow. . . . .   | 28 |
| 3.3 | Subcritical and supercritical bifurcations from zero amplitude. . . . .  | 31 |
| 4.1 | Phase portraits in the $r = 0$ plane. . . . .  | 37 |
| 4.2 | Stability diagram for rigid walls of the 3D system. . . . .  | 39 |
| 4.3 | Stability diagram for $\kappa = 1.1 \times 10^7$ of the 3D system. . . . .   | 40 |
| 4.4 | The continuation in $c$ of the Hopf bifurcating branch from $T_-$ into region III. Solid lines are stable periodic orbits. Supercritical period doubling bifurcations occur at (i) and (ii). . . . . | 41 |
| 4.5 | Orbits in the 3D system as examples of homoclinic ( $H0$ ) and heteroclinic connections ( $H1 - H4$ ). . . . .   | 43 |
| 4.6 | The heteroclinic connection $H4$ from a plane wave to a zero amplitude solution at $\Omega = 10$ and $c = 20$ . . . . .  | 44 |
| 4.7 | The heteroclinic connection $H3$ between two plane waves with different amplitudes at $\Omega = 10$ and $c = 9$ . . . . .  | 44 |

|      |   |    |
|------|---|----|
| 4.8  | The heteroclinic connection $H4$ from a zero amplitude solution to a plane wave at $\Omega = 10$ and $c = 9$ . . . . .                      | 45 |
| 4.9  | A nonperiodic orbit at $\Omega = 10$ and $c = 0.96$ for rigid wall boundary conditions. . . . .   | 46 |
| 4.10 | An attracting periodic orbit at $\Omega = 10$ and $c = 0.96$ for compliant wall boundary conditions ( $\kappa = 1.1 \times 10^7$ ). . . . . | 46 |
| 5.1  | Surface of two-dimensional finite amplitude traveling waves for rigid wall Poiseuille flow as a function of Reynolds number and wavenumber. | 48 |
| A.1  | Contour of $c_i$ in the $\alpha - Re$ plane. . . . .  | 52 |

# List of Tables

|     |  |    |
|-----|--|----|
| 3.1 | The Ginzburg-Landau coefficients for rigid walls. . . . .  | 29 |
| 3.2 | The effect of compliant walls on stability. . . . .  | 30 |
| 3.3 | The effect of damping on stability. . . . .  | 32 |
| 4.1 | The coefficients for the normal form of the Ginzburg-Landau equation<br>for rigid and compliant walls. . . . .                   | 35 |
| 4.2 | The numbers of stable and unstable eigenvalues of the critical points<br>in the regions of $\Omega - c$ parameter space. . . . . | 38 |
| A.1 | The location of the maximum value of $c_i$ in the $\alpha - Re$ plane. . . . .   | 51 |

# Chapter 1

## Introduction

The study of the interaction of incompressible shear flow with a compliant surface was initially motivated by the experiments of Kramer, who was himself motivated by the observations of R.W.L. Gwan [1948] and J.Gray [1957]. Using straightforward energy arguments, Gray concluded that for a dolphin to maintain the swimming speed of 22 miles per hour the flow of water over practically the entire animal's surface must be laminar. Kramer [1961,1965], who reported the drag-reducing capabilities of compliant coatings, conjectured that damping in the coating inhibited the development of Tollmien-Schlichting waves in the boundary layer, and, consequently, delayed or prevented the transition to turbulence. It should be noted, however, that despite much work by subsequent investigators no independent evidence has been obtained for the drag-reducing capabilities of Kramer's coatings (Carpenter and Garrad,[1985]).

The theoretical study of the effects of a flexible boundary on the hydrodynamic stability of a boundary layer was conducted by Benjamin [1960,1964], Landahl [1962], and Landahl and Kaplan [1965]. Similar studies for channel flow were conducted by Hains and Price [1962]. These investigators derived the linearized compliant boundary conditions, which is no mean feat since Korotkin [1965] and subsequent Soviet authors have apparently incorrectly implemented the no-slip condition at the compliant wall. In particular, let the displacement of the wall into the fluid be given by  $\eta$  and the displacement tangential to the undisturbed wall be given by  $\xi$ , as illustrated in Figure 1.1. The no-slip boundary conditions require that

$$\frac{\partial \xi}{\partial t} = u(x + \xi, y + \eta, t), \quad \frac{\partial \eta}{\partial t} = v(x + \xi, y + \eta, t), \quad (1.1)$$

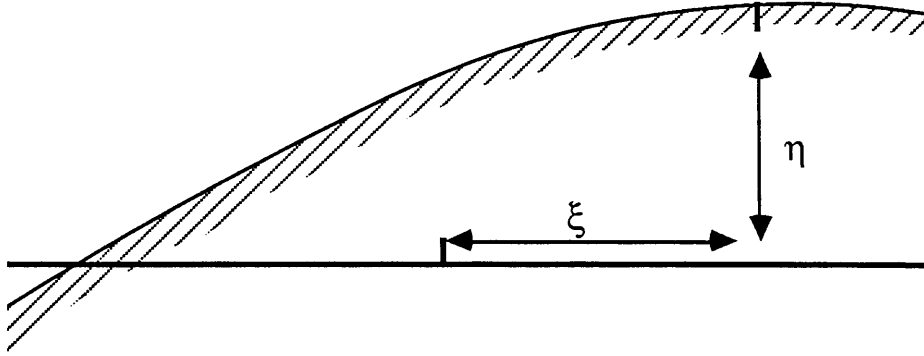


Figure 1.1: The definition of  $\eta$  and  $\xi$ .

at the walls. Expansion in a Taylor series about  $(\xi, \eta) = (0, 0)$  yields

$$\begin{aligned}\frac{\partial \xi}{\partial t} &= u(x, y_{wall}, t) + \xi \frac{\partial u}{\partial x} + \eta \frac{\partial u}{\partial y} + \text{h.o.t.} , \\ \frac{\partial \eta}{\partial t} &= v(x, y_{wall}, t) + \xi \frac{\partial v}{\partial x} + \eta \frac{\partial v}{\partial y} + \text{h.o.t.}\end{aligned}$$

Assuming that the wall has little freedom of movement in the  $x$ -direction, I take  $\xi \equiv 0$  , and, letting  $\eta$  be small, find that

$$\frac{\partial \eta}{\partial t} = v(x, y_{wall}, t) + \eta \frac{\partial v}{\partial y} , \quad \frac{\partial \xi}{\partial t} = 0 = u(x, y_{wall}, t) + \eta \frac{\partial u}{\partial y} , \quad (1.2)$$

where  $u$  and  $v$  are the fluid velocities evaluated at the location of the undisturbed wall. For  $\eta \equiv 0$  these linearized boundary conditions reduce to the usual no-slip boundary conditions

$$v(x, y_{wall}, t) = 0 , \quad u(x, y_{wall}, t) = 0 .$$

Following previous investigators, I introduce an additional boundary condition, one of which models how the compliant surface responds to the change in the pressure at the wall,  $\delta \tilde{p}_W$  :

$$-\tilde{B} \frac{\partial^4 \tilde{\eta}}{\partial x^4} + \tilde{T} \frac{\partial^2 \tilde{\eta}}{\partial x^2} - \tilde{\kappa} \tilde{\eta} - \rho_B \tilde{b} \frac{\partial^2 \tilde{\eta}}{\partial t^2} - \tilde{d} \frac{\partial \tilde{\eta}}{\partial t} = \delta \tilde{p}_W , \quad (1.3)$$

where  $\tilde{B}$  is the flexural rigidity of the surface,  $\tilde{T}$  the tension,  $\tilde{\kappa}$  the spring stiffness,  $\rho_B$  the mass density,  $\tilde{b}$  the wall thickness, and  $\tilde{d}$  the damping coefficient. I make no distinction between the mechanical pressure and the thermodynamical pressure in this incompressible flow. Non-dimensional variables can be chosen so that the principle of Squire's theorem still applies (as will be shown explicitly in the next chapter), a fact known to Benjamin [1964] but apparently not known to Riley, *et al.*, [1988], who scale their parameters quite differently.

To describe the linear stability analysis of parallel flow (Drazin and Reid [1981]), let  $U(y) = \partial\psi_0/\partial y$  be the undisturbed laminar velocity in the  $x$ -direction and  $(u, v) = (\psi_y, -\psi_x)$  be the infinitesimal perturbations to this velocity. Decomposing  $\psi$  into normal modes,

$$\psi = \phi(y)e^{i\alpha(x-ct)} ,$$

and substituting  $\psi_0 + \psi$  into the two-dimensional incompressible Navier-Stokes equations (shown explicitly in Chapter 2) yields, upon linearization,

$$\frac{i}{\alpha Re}(D^2 - \alpha^2)^2\phi + (U(y) - c)(D^2 - \alpha^2)\phi - \frac{d^2U}{dy^2}\phi = 0 , \quad (1.4)$$

the Orr-Sommerfeld equation, where  $D \equiv d/dy$ . For rigid walls, the boundary conditions become

$$\phi = 0 , \quad \phi' = 0 \quad \text{at the wall(s),}$$

and this equality is an eigenvalue equation for the complex wavespeed  $c = c(\alpha, Re)$ . When this equation is solved numerically, a single eigenfunction can be found for plane Poiseuille flow that has an eigenvalue  $c(\alpha, Re)$  whose imaginary part,  $c_i$ , becomes greater than zero in a region of the  $\alpha$ - $Re$  plane. The curve of marginal stability,  $c_i(\alpha, Re) = 0$ , is shown in Figure 1.2. It is still an open question whether such unsta-

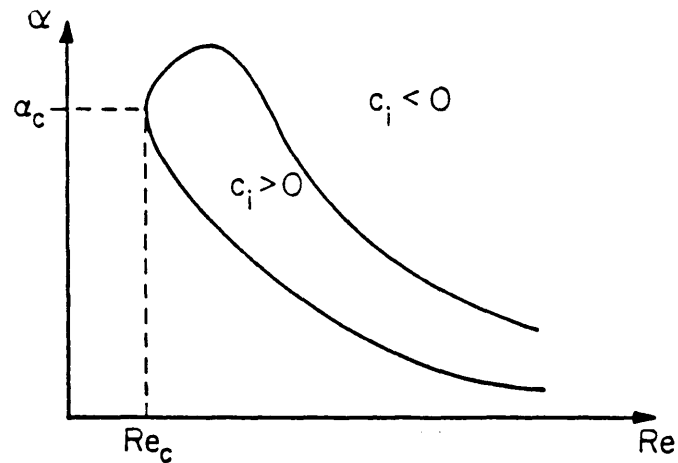


Figure 1.2: The curve of marginal stability.

ble regions exist for any of the other eigenfunctions. The minimum Reynolds number on the curve of marginal stability is the critical Reynolds number,  $Re_c$ , and its corresponding wavenumber is  $\alpha_c$ . A similar curve is found when the undisturbed flow is the Blasius boundary layer. An interesting result concerning the maximum value of the imaginary part of  $c(\alpha, Re)$  for this eigenfunction is discussed in Appendix A.

Assuming that the wall displacement  $\eta$  was of the same order of magnitude as the perturbation velocities, Benjamin extended conventional linear stability theory to parallel flows with compliant boundaries and found that for flows with no wall damping ( $\tilde{d} \equiv 0$  in equation 1.3) the neutral stability curves are shifted to lower wavenumbers and larger Reynolds numbers. Landahl's [1962] numerical examples, however, showed that the increase in the critical Reynolds number is modest. Benjamin also found that damping destabilizes these waves.

Benjamin identified three different types of wave disturbances, which he called classes A, B, and C. Class A disturbances are the Tollmien-Schlichting waves modified by the response of the compliant boundary (discussed above). Class B disturbances are associated with the free surface waves in the flexible wall. Class C instabilities are of Kelvin-Helmholtz type and arise when a class A wave coincides with a class B

wave in both wavespeed and wavelength. I will only be concerned with values of the wavelength, Reynolds number, and the flexibility parameters of equation 1.3 where class A wave disturbances are unstable (since I am concerned with the onset of the viscous instability). Class B instabilities depend fundamentally on surface flexibility and could exist in an inviscid fluid flow. It is not known whether a curve of marginal stability exists similar to Figure 1.2 where class B wave disturbances are unstable.

Carpenter and Garrad [1985,1986] numerically solved the Orr-Sommerfeld equation for a variety of compliant wall models and concluded that a transition delay is theoretically possible. However, this linear theory determines the stability of infinitesimal periodic disturbances. The Orr-Sommerfeld neutral curve is the zero amplitude intersection of a nonlinear neutral surface for finite amplitude two-dimensional waves (Bayly, *et al.*, [1988]), and it is this bifurcation from the zero amplitude waves to finite amplitude waves I wish to study.

In order to extend linear theory for rigid walls to account for small, but finite, amplitude disturbances in the flow, Stewartson and Stuart [1971] used a weakly nonlinear formulation based on the method of multiple scales. The stream function  $\psi$  is expanded about the base flow in both a power series in the small parameter  $\epsilon^{1/2}$  (proportional to the amplitude of the modulation) and in a harmonic series of the traveling wave found from linear theory at  $Re_c$ . In this analysis the perturbation stream function is given by

$$\psi = \epsilon^{1/2} \hat{A}(\xi, \tau) \phi(y) e^{i\alpha_c(x - c_c t)} + \text{c.c.} + O(\epsilon) \quad (1.5)$$

where  $\xi$  and  $\tau$  are the scaled slow streamwise coordinate and slow time, respectively, given by

$$\xi = \epsilon^{1/2}(x - c_g t), \quad \tau = \epsilon t. \quad (1.6)$$

The values for  $c_{cr}$ , the real part of the wavespeed at the critical point,  $\alpha_c$ , the wavenumber,  $c_g$ , the group velocity at which the energy of the modulation propagates, and  $\phi(y)$ , the Orr-Sommerfeld eigenfunction at the nose of the neutral stability curve where  $Re = Re_c$ , are found using the linear stability theory. In this expansion about the nose, the change in the Reynolds number is proportional to  $\epsilon$  and is given by

$$s_r(Re - Re_c) = \epsilon\sigma_r,$$

where  $\epsilon$  is greater than zero,  $\sigma_r$  is either  $+1$  or  $-1$ , and  $s_r$  is a fixed positive constant included for consistency with Stewartson and Stuart. The Ginzburg-Landau equation is found by substituting an expansion for  $\psi$  correct to order  $\epsilon^{3/2}$  into the Navier-Stokes equations and enforcing a solvability condition for the  $\epsilon^{3/2}$  inhomogeneous equation, thereby leading to:

$$\frac{\partial \hat{A}}{\partial \tau} = b \frac{\partial^2 \hat{A}}{\partial \xi^2} + \frac{s}{s_r} \sigma_r \hat{A} + \kappa \hat{A} |\hat{A}|^2. \quad (1.7)$$

The complex constants  $b$ ,  $s$ , and  $\kappa$  are also found numerically. In Chapter 3 I will derive equations for these constants for channel flow where the walls of the channel are compliant.

The normal form of the Ginzburg-Landau equation is found by rescaling  $\hat{A}$  to  $A$  and  $\xi$  to  $x$  (distinct from the fast scale  $x$ ) by letting

$$A = \sqrt{|\kappa_r|} \exp(-i\sigma_r s_i \tau / s_r) \hat{A}, \quad x = \xi / \sqrt{b_r}.$$

Upon this substitution I obtain

$$\frac{\partial A}{\partial \tau} = (a_r + ia_i) \frac{\partial^2 A}{\partial x^2} + \sigma_r A + (d_r + id_i) A |A|^2,$$

where, for  $b = b_r + ib_i$  and  $\kappa = \kappa_r + i\kappa_i$  in equation 1.7,

$$a_r = \frac{b_r}{|b_r|}, \quad a_i = \frac{b_i}{|b_r|}, \quad d_r = \frac{\kappa_r}{|\kappa_r|}, \quad d_i = \frac{\kappa_i}{|\kappa_r|}.$$

Landman [1987] studied a particular class of solutions of this equation of the form

$$A(x, \tau) = e^{-i\Omega\tau} \Phi(x - c\tau) ,$$

which he called quasisteady solutions, and found that their spatial variation may be periodic, quasiperiodic, or apparently chaotic. In Chapter 4 I will use this formalism to study the quasisteady solutions of the Ginzburg-Landau equation for compliant walls.

## Chapter 2

### Squire's Theorem

I would like to generalize a theorem of Squire [1933] that states that for any unstable disturbance in three dimensions there corresponds an unstable disturbance in two dimensions at a lower Reynolds number. An important consequence of this theorem is that to obtain the critical Reynolds number for periodic disturbances I need consider only two-dimensional disturbances. I am assuming that the undisturbed flow is given by

$$\tilde{U}(\tilde{y}) = U(1 - \tilde{y}^2/L^2)$$

where the channel walls are the parallel lines  $\tilde{y} = +L$  and  $\tilde{y} = -L$ . A similar theorem for the Blasius boundary layer requires only minor modifications. The motion of the lower wall (the proof is the same for either wall) in the  $\tilde{y}$ -direction,  $\tilde{\eta}$ , written in dimensional variables, is given by

$$\delta\tilde{p}_W = -\tilde{B}\nabla^4\tilde{\eta} + \tilde{T}\nabla^2\tilde{\eta} - \tilde{\kappa}\tilde{\eta} - \rho_B\tilde{b}\frac{\partial^2\tilde{\eta}}{\partial\tilde{t}^2} - \tilde{d}\frac{\partial\tilde{\eta}}{\partial\tilde{t}}, \quad (2.1)$$

where  $\tilde{B}$  is the flexural rigidity of the wall,  $\tilde{T}$  the tension,  $\tilde{\kappa}$  the spring stiffness,  $\rho_B$  the mass density,  $\tilde{b}$  the wall thickness,  $\tilde{d}$  the damping coefficient, and  $\delta\tilde{p}_W$  the change in the mechanical fluid pressure at the wall. Nondimensionalize the equation using the fluid density  $\rho$ , channel width  $2 \times L$ , centerline velocity  $U$ , and viscosity  $\mu$ :

$$\begin{aligned} x &= \frac{\tilde{x}}{L} & y &= \frac{\tilde{y}}{L} & z &= \frac{\tilde{z}}{L} & \eta &= \frac{\tilde{\eta}}{L} & t &= \frac{\tilde{t}U}{L} & \delta p &= \frac{\delta\tilde{p}_W}{\rho U^2} & Re &= \frac{UL\rho}{\mu} \\ B &= \frac{\tilde{B}\rho}{L\mu^2} & T &= \frac{\tilde{T}\rho L}{\mu^2} & \kappa &= \frac{\tilde{\kappa}L^3\rho}{\mu^2} & M &= \frac{\rho_B\tilde{b}}{\rho L} & d &= \frac{\tilde{d}L}{\mu} \end{aligned}$$

to obtain

$$\delta p = -\frac{B}{Re^2} \left[ \frac{\partial^4 \eta}{\partial x^4} + 2 \frac{\partial^4 \eta}{\partial x^2 \partial z^2} + \frac{\partial^4 \eta}{\partial z^4} \right] + \frac{T}{Re^2} \left[ \frac{\partial^2 \eta}{\partial x^2} + \frac{\partial^2 \eta}{\partial z^2} \right] - \frac{\kappa \eta}{Re^2} - M \frac{\partial^2 \eta}{\partial t^2} - \frac{d}{Re} \frac{\partial \eta}{\partial t}. \quad (2.2)$$

With these definitions I will prove

**Theorem 1 (Squire's Theorem for compliant boundaries)** *Given a set of compliancy parameters  $B, T, \kappa, M$ , and  $d$ , and an unstable periodic disturbance in three dimensions there corresponds an unstable periodic disturbance in two dimensions for the same compliancy parameters at a lower Reynolds number.*

Given the  $x$ -momentum equation,

$$\frac{\partial u}{\partial t} + u \frac{\partial u}{\partial x} + v \frac{\partial u}{\partial y} + w \frac{\partial u}{\partial z} + \frac{\partial P}{\partial x} = \frac{1}{Re} \left( \frac{\partial^2 u}{\partial x^2} + \frac{\partial^2 u}{\partial y^2} + \frac{\partial^2 u}{\partial z^2} \right),$$

the  $z$ -momentum equation,

$$\frac{\partial w}{\partial t} + u \frac{\partial w}{\partial x} + v \frac{\partial w}{\partial y} + w \frac{\partial w}{\partial z} + \frac{\partial P}{\partial z} = \frac{1}{Re} \left( \frac{\partial^2 w}{\partial x^2} + \frac{\partial^2 w}{\partial y^2} + \frac{\partial^2 w}{\partial z^2} \right),$$

and the boundary conditions at the walls,

$$\begin{aligned} 0 &= u + \eta \frac{\partial u}{\partial y}, \\ \frac{\partial \eta}{\partial t} &= v + \eta \frac{\partial v}{\partial y}, \\ 0 &= w + \eta \frac{\partial w}{\partial y}, \end{aligned}$$

I let  $U(y) = 1 - y^2$  be the undisturbed parallel flow (which vanishes at the wall) and impose a periodic disturbance:

$$\begin{aligned} p &= \hat{p}(y) e^{i(\alpha x + lz - c\alpha t)} + \frac{U''}{Re} x, \\ u &= U(y) + \hat{u}(y) e^{i(\alpha x + lz - c\alpha t)}, \\ v &= \hat{v}(y) e^{i(\alpha x + lz - c\alpha t)}, \\ w &= \hat{w}(y) e^{i(\alpha x + lz - c\alpha t)}. \end{aligned}$$

Letting

$$\eta = \hat{\eta} e^{i(\alpha x + lz - c\alpha t)}$$

at the wall, I substitute and linearize by assuming that the functions  $\hat{p}$ ,  $\hat{u}$ ,  $\hat{v}$ , and  $\hat{w}$  and the constant  $\hat{\eta}$  are all small quantities to obtain

$$-i\alpha c\hat{u} + i\alpha U(y)\hat{u} + \hat{v}U' + i\alpha\hat{p} = \frac{1}{Re}[\hat{u}'' - (\alpha^2 + l^2)\hat{u}] , \quad (2.3)$$

$$-i\alpha c\hat{w} + i\alpha U(y)\hat{w} + i l\hat{p} = \frac{1}{Re}[\hat{w}'' - (\alpha^2 + l^2)\hat{w}] , \quad (2.4)$$

and

$$\begin{aligned} 0 &= \hat{u} + \hat{\eta}U' , \\ -i\alpha c\hat{\eta} &= \hat{v} , \quad \text{and} \\ 0 &= \hat{w} \end{aligned}$$

at the wall. Evaluating the momentum equations at the wall gives

$$\begin{aligned} i\alpha\hat{p} &= \frac{1}{Re}[\hat{u}'' - (\alpha^2 + l^2)\hat{u}] + i\alpha c[\hat{u}(y) - \frac{\hat{v}}{i\alpha c}U'] , \\ i l\hat{p} &= \frac{1}{Re}[\hat{w}'' - (\alpha^2 + l^2)\hat{w}] . \end{aligned}$$

Eliminating  $\hat{\eta}$ ,

$$\begin{aligned} \hat{w} &= 0 , \\ \hat{u} - \frac{\hat{v}}{i\alpha c}U' &= 0 , \\ i\alpha\hat{p} &= \frac{1}{Re}[\hat{u}'' - (\alpha^2 + l^2)\hat{u}] \end{aligned}$$

at the wall. Substituting in equation 2.2 I obtain

$$\hat{p} = -\frac{\hat{v}}{i\alpha c} \left[ -(\alpha^2 + l^2)^2 \frac{B}{Re^2} - (\alpha^2 + l^2) \frac{T}{Re^2} - \frac{\kappa}{Re^2} + M\alpha^2 c^2 + i\alpha c \frac{d}{Re} \right] .$$

If I apply the Squire transformation,

$$m^2 \equiv \alpha^2 + l^2 , \quad \bar{u} \equiv \frac{\alpha\hat{u} + l\hat{w}}{m} , \quad \bar{Re} \equiv \frac{\alpha}{m} Re \leq Re , \quad \bar{p} \equiv \frac{m}{\alpha} \hat{p}$$

to the equations at the wall I obtain

$$\begin{aligned}\bar{u} - \frac{\hat{v}}{imc}U' &= 0, \\ im\bar{p} &= \frac{1}{\bar{Re}}(\bar{u}'' - m^2\bar{u}), \\ \bar{p} &= -\frac{\hat{v}}{imc}\left[-m^4\frac{B}{\bar{Re}^2} - m^2\frac{T}{\bar{Re}^2} - \frac{\kappa}{\bar{Re}^2} + Mm^2c^2 + imc\frac{d}{\bar{Re}^2}\right],\end{aligned}$$

which are the boundary conditions for two-dimensional disturbances for  $\bar{u}$ ,  $\hat{v}$ ,  $\bar{p}$ , the wavenumber  $m$ , and the Reynolds number  $\bar{Re}$ . If I apply the Squire transformation to equations 2.3 and 2.4 I obtain

$$-imc\bar{u} + imU(y)\bar{u} + \hat{v}U' + im\bar{p} = \frac{1}{\bar{Re}}[\bar{u}'' - m^2\bar{u}],$$

the  $x$ -momentum equation for  $\bar{u}$ , and the continuity equation,

$$i\alpha\hat{u} + \frac{\partial\hat{v}}{\partial y} + i\ell\hat{w} = 0,$$

becomes the two-dimensional continuity equation

$$im\bar{u} + \frac{\partial\hat{v}}{\partial y} = 0.$$

Consequently, for fixed  $B$ ,  $T$ ,  $\kappa$ ,  $M$ , and  $d$ , the minimum critical Reynolds number occurs for a two-dimensional disturbance, and it is reasonable to use a two-dimensional model to study the onset of the instability of the flow.

# Chapter 3

## Ginzburg-Landau equation

In this chapter I will present the details of a model of the flow over a compliant surface and study the stability of that flow. First I will derive the Ginzburg-Landau equation for channel flow with compliant walls, and then I will discuss what properties of the finite amplitude steady waves that bifurcate from channel flow can be inferred from this weakly nonlinear model.

### 3.1 Derivation of the Ginzburg-Landau equation

In this derivation of the Ginzburg-Landau equation I follow the original derivation of Stewartson and Stuart [1971] and that of Davey, *et al.*, [1974]. Several of the formulae used in this derivation will be used to find the boundary conditions of compliant walls.

As a notational convenience I define  $P^{(1)}$  and  $P^{(2)}$  as the pressure gradients in the  $x$  and  $y$  directions, respectively, and relate these functions by the consistency equation

$$\frac{\partial P^{(1)}}{\partial y} = \frac{\partial P^{(2)}}{\partial x} . \quad (3.1)$$

This equation, along with the two-dimensional Navier-Stokes equations,

$$\begin{aligned} \frac{\partial u}{\partial t} + u \frac{\partial u}{\partial x} + v \frac{\partial u}{\partial y} + P^{(1)} &= \frac{1}{Re} \left( \frac{\partial^2 u}{\partial x^2} + \frac{\partial^2 u}{\partial y^2} \right) , \\ \frac{\partial v}{\partial t} + u \frac{\partial v}{\partial x} + v \frac{\partial v}{\partial y} + P^{(2)} &= \frac{1}{Re} \left( \frac{\partial^2 v}{\partial x^2} + \frac{\partial^2 v}{\partial y^2} \right) \\ \frac{\partial u}{\partial x} + \frac{\partial v}{\partial y} &= 0 , \end{aligned}$$

are the equations of motion. These equations must be modified in the method of

multiple scales to conform with equation 1.6 by making the substitutions

$$\frac{\partial}{\partial t} \longrightarrow \frac{\partial}{\partial t} + \epsilon \frac{\partial}{\partial \tau} - c_g \epsilon^{1/2} \frac{\partial}{\partial \xi}, \quad \frac{\partial}{\partial x} \longrightarrow \frac{\partial}{\partial x} + \epsilon^{1/2} \frac{\partial}{\partial \xi}.$$

Letting  $\alpha_c$  be the critical wavenumber on the curve of marginal stability and  $c_{cr}$  be the real part of the wavespeed at the nose (Figure 1.2), expand the velocities and pressure gradients in a harmonic series of the form

$$u = u_0 + u_1 E + \bar{u}_1 \bar{E} + u_2 E^2 + \bar{u}_2 \bar{E}^2 \quad E = e^{i\alpha_c(x - c_{cr}t)}$$

and similarly for  $v$ ,  $P^{(1)}$ , and  $P^{(2)}$ . The overbar denotes the complex conjugate. The functions  $u_0$ ,  $u_1$ , and  $u_2$  are functions of  $y$ ,  $\xi$ , and  $\tau$  only. The Ginzburg-Landau equation is found from a solvability condition at order  $\epsilon^{3/2}$ , so I let:

$$\begin{aligned} u_0 &= U[(1 - y^2) + \epsilon u_{20} + O(\epsilon^{3/2})] \\ u_1 &= U[\epsilon^{1/2} u_{11} + \epsilon u_{21} + \epsilon^{3/2} u_{31} + O(\epsilon^2)] \\ u_2 &= U[\epsilon u_{22} + O(\epsilon^{3/2})] \\ v_0 &= U[\epsilon v_{20} + O(\epsilon^{3/2})] \\ v_1 &= U[\epsilon^{1/2} v_{11} + \epsilon v_{21} + \epsilon^{3/2} v_{31} + O(\epsilon^2)] \\ v_2 &= U[\epsilon v_{22} + O(\epsilon^{3/2})] \\ P_0^{(1)} &= U[-2/Re + \epsilon P_{20}^{(1)} + O(\epsilon^{3/2})] \\ P_1^{(1)} &= U[\epsilon^{1/2} P_{11}^{(1)} + \epsilon P_{21}^{(1)} + \epsilon^{3/2} P_{31}^{(1)} + O(\epsilon^2)] \\ P_2^{(1)} &= U[\epsilon P_{22}^{(1)} + O(\epsilon^{3/2})] \\ P_0^{(2)} &= U[\epsilon P_{20}^{(2)} + O(\epsilon^{3/2})] \\ P_1^{(2)} &= U[\epsilon^{1/2} P_{11}^{(2)} + \epsilon P_{21}^{(2)} + \epsilon^{3/2} P_{31}^{(2)} + O(\epsilon^2)] \\ P_2^{(2)} &= U[\epsilon P_{22}^{(2)} + O(\epsilon^{3/2})] \end{aligned}$$

Plane Poiseuille flow is chosen for the base flow because it is a truly parallel flow and can be exactly described by a polynomial in  $y$  . These expressions are substituted into the two-dimensional Navier-Stokes equations and coefficients of  $\epsilon^{n/2} E^m$  ( $n, m = 0, 1, 2, \dots$ ) are equated to zero.

From the coefficient of  $\epsilon^{1/2} E$  I obtain

$$\begin{aligned} u_{11} &= \frac{i}{\alpha} \frac{\partial v_{11}}{\partial y}, & \frac{\partial P_{11}^{(1)}}{\partial y} &= i\alpha P_{11}^{(2)}, \\ i\alpha(1 - y^2 - c) u_{11} - 2yv_{11} + P_{11}^{(1)} &= \frac{1}{Re}(D^2 - \alpha^2) u_{11}, \\ i\alpha(1 - y^2 - c) v_{11} + P_{11}^{(2)} &= \frac{1}{Re}(D^2 - \alpha^2) v_{11}, \end{aligned}$$

where, here and throughout, I let  $D \equiv d/dy$  and write  $\alpha, c$  for the more cumbersome  $\alpha_c, c_{cr}$  . Eliminating the pressure gradients and  $u_{11}$  in the above equations gives

$$\mathcal{L} v_{11} \equiv \frac{i}{\alpha Re}(D^2 - \alpha^2)^2 v_{11} + (1 - y^2 - c)(D^2 - \alpha^2)v_{11} + 2v_{11} = 0,$$

the Orr-Sommerfeld equation.

From the coefficient  $\epsilon E$  I obtain

$$\begin{aligned} u_{12} &= \frac{i}{\alpha} \frac{\partial v_{12}}{\partial y} - \frac{1}{\alpha^2} \frac{\partial^2 v_{11}}{\partial \xi \partial y} \\ \frac{\partial P_{12}^{(1)}}{\partial y} &= i\alpha P_{12}^{(2)} + \frac{\partial P_{11}^{(2)}}{\partial \xi} \\ i\alpha(1 - y^2 - c)u_{12} + P_{12}^{(1)} - (1 - y^2)\frac{\partial u_{11}}{\partial \xi} - c_g \frac{\partial u_{11}}{\partial \xi} - 2yv_{12} &= \frac{1}{Re} \left[ (D^2 - \alpha^2)u_{12} + 2i\alpha \frac{\partial u_{11}}{\partial \xi} \right] \\ i\alpha(1 - y^2 - c)v_{12} + P_{12}^{(2)} + (1 - y^2)\frac{\partial v_{11}}{\partial \xi} - c_g \frac{\partial v_{11}}{\partial \xi} &= \frac{1}{Re} \left[ (D^2 - \alpha^2)v_{12} + 2i\alpha \frac{\partial v_{11}}{\partial \xi} \right], \end{aligned}$$

which implies that

$$\begin{aligned} \mathcal{L}v_{12} &= \frac{c_g}{i\alpha} \frac{\partial}{\partial \xi} (D^2 - \alpha^2)v_{11} \\ &+ \frac{1}{i\alpha} \frac{\partial}{\partial \xi} \left[ -\left(1 - y^2 - \frac{4i\alpha}{Re}\right)(D^2 - \alpha^2)v_{11} + 2\alpha^2(1 - y^2 - c)v_{11} - 2v_{11} \right]. \end{aligned} \quad (3.2)$$

The solvability condition for this equation gives the value of  $c_g$ , but I have found this constant using a method discussed in Appendix B.

From the coefficient  $\epsilon E^2$  I obtain

$$\begin{aligned} u_{22} &= \frac{i}{2\alpha} \frac{\partial v_{22}}{\partial y}, & \frac{\partial P_{22}^{(1)}}{\partial y} &= 2i\alpha P_{22}^{(2)}, \\ 2i\alpha(1 - y^2 - c)u_{22} - 2yv_{22} + i\alpha u_{11}^2 + v_{11} \frac{\partial u_{11}}{\partial y} + P_{22}^{(1)} &= \frac{1}{Re}(D^2 - \alpha^2)u_{22}, \\ 2i\alpha(1 - y^2 - c)v_{22} + i\alpha u_{11}v_{11} + v_{11} \frac{\partial v_{11}}{\partial y} + P_{22}^{(2)} &= \frac{1}{Re}(D^2 - \alpha^2)v_{22}. \end{aligned}$$

Eliminating the pressure gradients,  $u_{22}$ , and  $u_{11}$  in the above equations gives

$$\begin{aligned} \frac{i}{2\alpha Re}(D^2 - 4\alpha^2)^2 v_{22} + (1 - y^2 - c)(D^2 - 4\alpha^2)v_{22} + 2v_{22} &= \\ -\frac{i}{\alpha} \left[ \frac{\partial v_{11}}{\partial y} \frac{\partial^2 v_{11}}{\partial y^2} - v_{11} \frac{\partial^3 v_{11}}{\partial y^3} \right]. \end{aligned} \quad (3.3)$$

From the coefficient  $\epsilon E^0$  I obtain (omitting the formula from the  $y$ -momentum equation)

$$\begin{aligned} \frac{\partial v_{20}}{\partial y} &= 0, & \frac{\partial P_{20}^{(1)}}{\partial y} &= 0, \\ -2yv_{20} + v_{11} \frac{\partial \bar{u}_{11}}{\partial y} + \bar{v}_{11} \frac{\partial u_{11}}{\partial y} + P_{20}^{(1)} &= \frac{1}{Re} \frac{\partial^2 u_{20}}{\partial y^2}. \end{aligned}$$

For rigid walls the no-slip boundary conditions require that  $v_{20}(\pm 1) = 0$ , and since  $\partial v_{20}/\partial y = 0$  throughout the fluid, I find that  $v_{20} \equiv 0$ . In the next section I will show that  $v_{20} \equiv 0$  for flexible walls as well. Consequently, I conclude  $P_{20}^{(1)}$  is a function of  $\xi$  and  $\tau$  only and, eliminating  $u_{11}$ , I have

$$\frac{1}{Re} \frac{\partial^2 u_{20}}{\partial y^2} = P_{20}^{(1)} + \frac{1}{i\alpha} \left( v_{11} \frac{\partial^2 \bar{v}_{11}}{\partial y^2} - \bar{v}_{11} \frac{\partial^2 v_{11}}{\partial y^2} \right). \quad (3.4)$$

From the coefficient  $\epsilon^{3/2}E$  I obtain

$$\begin{aligned}
 u_{13} &= \frac{i}{\alpha} \frac{\partial v_{13}}{\partial y} - \frac{1}{\alpha^2} \frac{\partial^2 v_{12}}{\partial \xi \partial y} - \frac{i}{\alpha^3} \frac{\partial^3 v_{11}}{\partial^2 \xi \partial y} \\
 \frac{\partial P_{13}^{(1)}}{\partial y} &= i\alpha P_{13}^{(2)} + \frac{\partial P_{12}^{(2)}}{\partial \xi} \\
 i\alpha(1-y^2-c)u_{13} - 2yv_{13} + P_{13}^{(1)} + (1-y^2)\frac{\partial u_{12}}{\partial \xi} - c_g\frac{\partial u_{12}}{\partial \xi} + \frac{\partial u_{11}}{\partial \tau} + i\alpha u_{20}u_{11} \\
 + v_{11}\frac{\partial u_{20}}{\partial y} + i\alpha u_{22}\bar{u}_{11} + v_{22}\frac{\partial \bar{u}_{11}}{\partial y} + \bar{v}_{11}\frac{\partial u_{22}}{\partial y} &= \frac{1}{Re} \left[ (D^2 - \alpha^2)u_{13} + 2i\alpha\frac{\partial u_{12}}{\partial \xi} + \frac{\partial^2 u_{11}}{\partial \xi^2} \right] \\
 i\alpha(1-y^2-c)v_{13} + (1-y^2)\frac{\partial v_{12}}{\partial \xi} - c_g\frac{\partial v_{12}}{\partial \xi} + \frac{\partial v_{11}}{\partial \tau} + i\alpha u_{20}v_{11} - i\alpha u_{22}\bar{v}_{11} \\
 + 2i\alpha\bar{u}_{11}v_{22} + \bar{v}_{11}\frac{\partial v_{22}}{\partial y} + v_{22}\frac{\partial \bar{v}_{11}}{\partial y} + P_{13}^{(2)} &= \frac{1}{Re} \left[ (D^2 - \alpha^2)v_{13} + 2i\alpha\frac{\partial v_{12}}{\partial \xi} + \frac{\partial^2 v_{11}}{\partial \xi^2} \right].
 \end{aligned}$$

Eliminating the pressure gradients,  $u_{11}$ ,  $u_{12}$ , and  $u_{22}$  gives

$$\begin{aligned}
 \mathcal{L}v_{13} &= \frac{i}{\alpha} \frac{\partial}{\partial \tau} (D^2 - \alpha^2)v_{11} + \left[ u_{20}(D^2 - \alpha^2)v_{11} - v_{11}\frac{\partial^2 u_{20}}{\partial y^2} \right] + \\
 \frac{i}{2\alpha} \left[ \frac{\partial v_{22}}{\partial y}(D^2 - \alpha^2)\bar{v}_{11} + 2v_{22}(D^2 - \alpha^2)\frac{\partial \bar{v}_{11}}{\partial y} - 2\frac{\partial \bar{v}_{11}}{\partial y}(D^2 - 4\alpha^2)v_{22} \right. \\
 &\quad \left. - \bar{v}_{11}(D^2 - 4\alpha^2)\frac{\partial v_{22}}{\partial y} \right] \quad (3.5) \\
 - \frac{i}{\alpha} \frac{\partial}{\partial \xi} \left[ -(1-y^2-c_g - \frac{4i\alpha}{Re})(D^2 - \alpha^2)v_{12} + 2\alpha^2(1-y^2-c)v_{12} - 2v_{12} \right] \\
 - \frac{1}{\alpha^2} \frac{\partial^2}{\partial \xi^2} \left[ (c - c_g - \frac{2i\alpha}{Re})(D^2 + \alpha^2)v_{11} + (1-y^2-c)D^2v_{11} + 2v_{11} \right].
 \end{aligned}$$

This equation has a solution only if the right-hand side satisfies a certain integral condition; this integral condition gives the Ginzburg-Landau equation.

If I let

$$\begin{aligned}
 v_{11}(y, \xi, \tau) &= -i\alpha A(\xi, \tau) \psi(y), & v_{22}(y, \xi, \tau) &= -2i\alpha A^2 \psi_2(y), \\
 v_{12}(y, \xi, \tau) &= -\frac{\partial A}{\partial \xi} (\alpha\psi_{10} + \psi),
 \end{aligned}$$

then equation 3.5 becomes

$$\begin{aligned} \mathcal{L} v_{13} = & \frac{\partial A}{\partial \tau} (D^2 - \alpha^2) \psi + i\alpha A \left[ u_{20} (D^2 - \alpha^2) \psi - \psi \frac{\partial u_{20}}{\partial y^2} \right] - \\ & i\alpha A |A|^2 \left[ \frac{\partial \psi_2}{\partial y} (D^2 - \alpha^2) \bar{\psi} + 2\psi_2 (D^2 - \alpha^2) \frac{\partial \bar{\psi}}{\partial y} - 2 \frac{\partial \bar{\psi}}{\partial y} (D^2 - 4\alpha^2) \psi_2 - \bar{\psi} (D^2 - 4\alpha^2) \frac{\partial \psi_2}{\partial y} \right] \\ & + i \frac{\partial^2 A}{\partial \xi^2} \left[ - (1 - y^2 - c_g - \frac{4i\alpha}{Re}) (D^2 - \alpha^2) (\psi_{10} + \frac{\psi}{\alpha}) + 2\alpha^2 (1 - y^2 - c) (\psi_{10} + \frac{\psi}{\alpha}) \right. \\ & \left. - 2(\psi_{10} + \frac{\psi}{\alpha}) + (c - c_g - \frac{2i\alpha}{Re}) (D^2 + \alpha^2) \psi + (1 - y^2 - c) D^2 \psi + 2\psi \right]. \end{aligned}$$

When the walls are rigid, both  $v_{13}$  and  $\psi$  have the same boundary conditions, viz.,

$$\psi(\pm 1) = 0, \quad \frac{\partial \psi}{\partial y}(\pm 1) = 0, \quad v_{13}(\pm 1) = 0, \quad \frac{\partial v_{13}}{\partial y}(\pm 1) = 0;$$

furthermore, the adjoint to the Orr-Sommerfeld eigenfunction,  $\Phi(y)$ , where

$$\begin{aligned} \frac{i}{\alpha Re} (D^2 - \alpha^2)^2 \Phi + (1 - y^2 - c) (D^2 - \alpha^2) \Phi - 4y D\Phi = 0, \\ \Phi(\pm 1) = 0, \quad \frac{\partial \Phi}{\partial y}(\pm 1) = 0, \end{aligned}$$

is also adjoint to the homogeneous equation

$$\mathcal{L} v_{13} = 0. \tag{3.6}$$

However, when  $\psi$  and  $v_{13}$  have different boundary conditions,  $\Phi$  is no longer adjoint to equation 3.6, and the calculation of the Ginzburg-Landau coefficients is not as straightforward. This calculation will be examined in more detail in the next section.

Making these substitutions into equation 3.4 gives

$$\frac{\partial^2 u_{20}}{\partial y^2} = Re \left[ P_{20}^{(1)} + i\alpha |A|^2 \frac{\partial}{\partial y} \left( \bar{\psi} \frac{\partial \psi}{\partial y} - \psi \frac{\partial \bar{\psi}}{\partial y} \right) \right]$$

and letting  $u_{20}(\pm 1) = 0$  (rigid walls) yields

$$u_{20}(y, \xi, \tau) = \frac{3}{2} \hat{P}(1 - y^2) + |A|^2 (S(y) - \frac{3}{2} S_0(1 - y^2)),$$

$$\begin{aligned}
 S(y) &\equiv i\alpha Re \int_{+1}^y (\bar{\psi} \frac{\partial \psi}{\partial y} - \psi \frac{\partial \bar{\psi}}{\partial y}) dy , \\
 \hat{P} &\equiv S_0 |A|^2 - \frac{Re}{3} P_{20}^{(1)} , \\
 S_0 &\equiv \int_0^1 S(y) dy .
 \end{aligned}$$

This choice of variables is motivated by the fact that

$$\int_0^1 u_{20} dy = \hat{P} ,$$

and the time averaged fluid flux,  $Q$  , is given by

$$Q \equiv \int_{-1}^{+1} u_0 dy = \int_{-1}^{+1} U[1 - y^2 + \epsilon u_{20} + O(\epsilon^{3/2})] dy = \frac{4U}{3} + \epsilon 2U\hat{P} + O(\epsilon^{3/2}) .$$

## 3.2 The Compliant Boundary Conditions

The only known unstable eigenfunction of the Orr-Sommerfeld equation for channel flow is symmetric about the center of the channel ( $y = 0$ ), as are its adjoint,  $\Phi(y)$  , and the function  $\psi_{10}(y)$  . Taking advantage of that symmetry, I will derive the compliant boundary conditions for the lower wall alone. The symmetry implies that the equations for the walls are identical except when the response of the wall to the mechanical pressure is specified. In particular, if I define  $\tilde{\eta}$  , the displacement of the wall in the  $y$ -direction, at the upper and lower walls as shown in Figure 3.1 and  $\delta\tilde{p}_W$  as the change in the pressure at the wall, then for a simple Hooke's law wall I have

$$\delta\tilde{p}_W = +\tilde{\kappa}\tilde{\eta} \quad \text{upper wall} \quad \delta\tilde{p}_W = -\tilde{\kappa}\tilde{\eta} \quad \text{lower wall} ,$$

since when the pressure change is positive I expect  $\tilde{\eta}$  at the upper wall to increase and  $\tilde{\eta}$  at the lower wall to decrease. I will now use the dimensionless variables defined in Chapter 2.

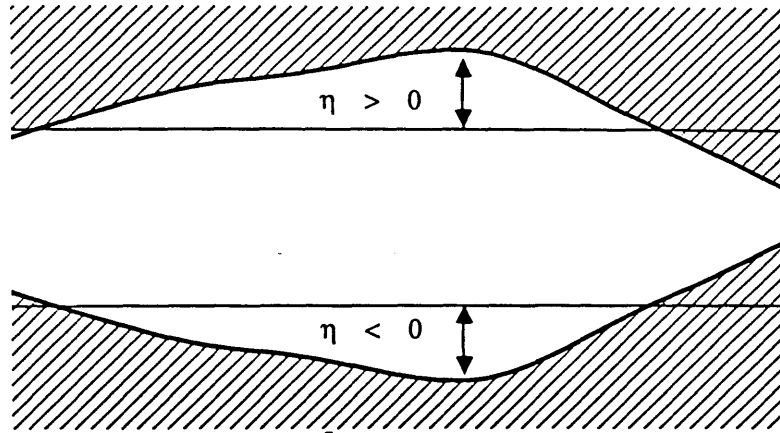


Figure 3.1: The displacement of the upper and lower walls.

For undisturbed Poiseuille flow with fluid velocity  $U(y) = 1 - y^2$ , let the upper wall be the line  $y = +1$  and the lower wall  $y = -1$ . Expand  $\eta$  in a harmonic series

$$\eta = \eta_0 + \eta_1 E + \bar{\eta}_1 \bar{E} + \eta_2 E^2 + \bar{\eta}_2 \bar{E}^2 \quad E = e^{i\alpha_c(x - c_c t)},$$

where the  $\eta_k$  are functions of  $y$ ,  $\xi$ , and  $\tau$  only, and overbar denotes complex conjugation. Expand each of these in a power series in  $\epsilon^{1/2}$ :

$$\begin{aligned} \eta_0 &= 0 && \text{by hypothesis} \\ \eta_1 &= \epsilon^{1/2} \eta_{11} + \epsilon \eta_{21} + \epsilon^{3/2} \eta_{31} + O(\epsilon^2) \\ \eta_2 &= \epsilon \eta_{22} + O(\epsilon^{3/2}). \end{aligned}$$

It is necessary to assume that the wall displacement due to the changes in the mean flow,  $\eta_0$ , is identically zero in order to satisfy the continuity equation. This assumption is equivalent to requiring a fictitious force opposing the mean pressure on the walls at the  $O(\epsilon)$  level.

Expanding the no-slip boundary conditions (equation 1.1) in a Taylor series gives

$$\begin{aligned} 0 &= u + \eta \frac{\partial u}{\partial y} + \frac{\eta^2}{2} \frac{\partial^2 u}{\partial y^2} + O(\epsilon^2) \\ \frac{\partial \eta}{\partial t} + \epsilon \frac{\partial \eta}{\partial \tau} - c_g \epsilon^{1/2} \frac{\partial \eta}{\partial \xi} &= v + \eta \frac{\partial v}{\partial y} + \frac{\eta^2}{2} \frac{\partial^2 v}{\partial y^2} + O(\epsilon^2). \end{aligned}$$

For simplicity I will assume a Hooke's law with no damping,

$$\delta p = -\frac{\kappa}{Re^2} \eta \quad (\text{lower wall}) .$$

The pressure gradient is related to the lower wall displacement by the equation

$$P^{(1)} = \frac{\partial P}{\partial x} + \epsilon^{1/2} \frac{\partial P}{\partial \xi} = -\frac{\kappa}{Re^2} \left( \frac{\partial \eta}{\partial x} + \epsilon^{1/2} \frac{\partial \eta}{\partial \xi} \right) ,$$

with the opposite sign at the upper wall.

From the coefficient of  $\epsilon^{1/2}E$  I obtain

$$-i\alpha c \eta_{11} = v_{11} , \quad 0 = u_{11} + 2 \eta_{11} , \quad P_{11}^{(1)} = -\frac{\kappa}{Re^2} (i\alpha \eta_{11}) ,$$

and, eliminating  $\eta_{11}$  ,

$$0 = u_{11} + \frac{2}{c} \frac{v_{11}}{(-i\alpha)} , \quad P_{11}^{(1)} = -\frac{\kappa}{c Re^2} v_{11} .$$

The continuity equation and  $x$ -momentum equation hold throughout the fluid, and, evaluating these equations at the lower wall,

$$\frac{\partial v_{11}}{\partial y} = -i\alpha u_{11} , \quad P_{11}^{(1)} = \frac{1}{Re} \left[ \frac{\partial^2 u_{11}}{\partial y^2} - \alpha^2 u_{11} \right] ,$$

I can eliminate the variables  $u_{11}$  and  $P_{11}^{(1)}$  to find

$$0 = c \frac{\partial v_{11}}{\partial y} + 2 v_{11} \quad 0 = \frac{Re}{\kappa} \left[ c \frac{\partial^3 v_{11}}{\partial y^3} + 2\alpha^2 v_{11} \right] + i\alpha v_{11} .$$

Here I have used the fact that the derivatives of the continuity equation are also valid at the wall. Similarly, at the upper wall,

$$0 = c \frac{\partial v_{11}}{\partial y} - 2 v_{11} , \quad 0 = \frac{Re}{\kappa} \left[ -c \frac{\partial^3 v_{11}}{\partial y^3} + 2\alpha^2 v_{11} \right] + i\alpha v_{11} ,$$

and the symmetry of  $v_{11}(y)$  about the center of the channel is preserved.

From the coefficient of  $\epsilon E^0$  I obtain

$$\begin{aligned} 0 &= v_{20} + \eta_{11} \frac{\partial \bar{v}_{11}}{\partial y} + \bar{\eta}_{11} \frac{\partial v_{11}}{\partial y} , \\ 0 &= u_{20} + \eta_{11} \frac{\partial \bar{u}_{11}}{\partial y} + \bar{\eta}_{11} \frac{\partial u_{11}}{\partial y} - 2 \eta_{11} \bar{\eta}_{11} . \end{aligned}$$

Substituting the expressions for  $\eta_{11}$  ,  $v_{11}$  , and  $u_{11}$  I find that

$$v_{20} = 0 , \quad u_{20} + \frac{1}{c} \left[ \frac{v_{11}}{(-i\alpha)} \frac{\partial \bar{u}_{11}}{\partial y} + \frac{\bar{v}_{11}}{i\alpha} \frac{\partial u_{11}}{\partial y} \right] - \frac{2}{c^2} \frac{v_{11}}{(-i\alpha)} \frac{\bar{v}_{11}}{i\alpha} = 0 ,$$

and, since  $\partial v_{20} / \partial y = 0$  throughout the fluid,

$$v_{20} \equiv 0 .$$

Using the notation of the previous section, I have

$$\begin{aligned} u_{20}(y) &= \frac{3}{2} \hat{P} (1 - y^2) + |A|^2 (S(y) - \frac{3}{2} S_0 (1 - y^2)) , \\ \frac{\partial S}{\partial y}(y) &= i\alpha \operatorname{Re} \left( \bar{\psi} \frac{\partial \psi}{\partial y} - \psi \frac{\partial \bar{\psi}}{\partial y} \right) , \\ S(-1) &= \frac{2}{c^2} \psi \bar{\psi} - \frac{1}{c} \left( \psi \frac{\partial^2 \bar{\psi}}{\partial y^2} + \bar{\psi} \frac{\partial^2 \psi}{\partial y^2} \right) , \\ \hat{P} &\equiv S_0 |A|^2 - \frac{\operatorname{Re} \epsilon}{3} P_{20}^{(1)} , \\ S_0 &\equiv \int_0^1 S(y) dy , \end{aligned}$$

where I have used the symmetry of  $S(y)$  , and

$$\begin{aligned} \mathcal{L} \psi &\equiv \frac{i}{\alpha \operatorname{Re}} (D^2 - \alpha^2)^2 \psi + (1 - y^2 - c)(D^2 - \alpha^2) \psi + 2\psi = 0 \\ 0 &= c \frac{\partial \psi}{\partial y} - 2\psi \quad 0 = i\alpha \psi + \frac{\operatorname{Re} \epsilon}{\kappa} (2\alpha^2 \psi - c \frac{\partial^3 \psi}{\partial y^3}) \quad \text{at } y = +1 \\ 0 &= c \frac{\partial \psi}{\partial y} + 2\psi \quad 0 = i\alpha \psi + \frac{\operatorname{Re} \epsilon}{\kappa} (2\alpha^2 \psi + c \frac{\partial^3 \psi}{\partial y^3}) \quad \text{at } y = -1 . \end{aligned}$$

Defining the adjoint  $\Phi$  by

$$\int_{-1}^{+1} \Phi \mathcal{L} \psi dy = \int_{-1}^{+1} \psi \mathcal{L}^\dagger \Phi dy$$

implies that

$$\begin{aligned}\mathcal{L}^\dagger \Phi &\equiv \frac{i}{\alpha Re} (D^2 - \alpha^2)^2 \Phi + (1 - y^2 - c)(D^2 - \alpha^2)\Phi - 4y D\Phi = 0 \\ \frac{\partial \Phi}{\partial y} = 0 &\quad i\alpha \Phi - \frac{Re}{\kappa} (2\alpha^2 \Phi - 2\frac{\partial^2 \Phi}{\partial y^2} + c\frac{\partial^3 \Phi}{\partial y^3}) = 0 \quad \text{at } y = +1 \\ \frac{\partial \Phi}{\partial y} = 0 &\quad i\alpha \Phi - \frac{Re}{\kappa} (2\alpha^2 \Phi - 2\frac{\partial^2 \Phi}{\partial y^2} - c\frac{\partial^3 \Phi}{\partial y^3}) = 0 \quad \text{at } y = -1 ,\end{aligned}$$

and the adjoint is symmetric with respect to  $y = 0$ .

From the coefficient of  $\epsilon E^2$  I obtain

$$\begin{aligned}-2i\alpha c \eta_{22} &= v_{22} + \eta_{11} \frac{\partial v_{11}}{\partial y} \\ 0 &= u_{22} + 2\eta_{22} + \eta_{11} \frac{\partial u_{11}}{\partial y} - \eta_{11}^2 \\ P_{22}^{(1)} &= -\frac{\kappa}{Re^2} (2i\alpha \eta_{22}) .\end{aligned}$$

Eliminating  $\eta_{22}$  and  $\eta_{11}$  gives

$$\begin{aligned}2i\alpha c u_{22} &= 2v_{22} + \frac{4i\alpha}{c^2} \left(\frac{v_{11}}{-i\alpha}\right)^2 + 2v_{11} \frac{\partial u_{11}}{\partial y} + \frac{2i\alpha}{c} \left(\frac{v_{11}}{-i\alpha}\right)^2 \\ P_{22}^{(1)} &= \frac{\kappa}{c Re^2} \left[ v_{22} + \frac{2i\alpha}{c^2} \left(\frac{v_{11}}{-i\alpha}\right)^2 \right] .\end{aligned}$$

Evaluating the  $x$ -momentum equation at the wall

$$P_{22}^{(1)} = \frac{1}{Re} \left( \frac{\partial^2 u_{22}}{\partial y^2} - 4\alpha^2 u_{22} \right) + 2i\alpha c u_{22} - 2v_{22} - i\alpha u_{11}^2 - v_{11} \frac{\partial u_{11}}{\partial y} ,$$

and eliminating  $P_{22}^{(1)}$  gives

$$\frac{\kappa}{c Re^2} \left[ v_{22} + \frac{2i\alpha}{c^2} \left(\frac{v_{11}}{-i\alpha}\right)^2 \right] = \frac{1}{Re} \left( \frac{\partial^2 u_{22}}{\partial y^2} - 4\alpha^2 u_{22} \right) + v_{11} \frac{\partial u_{11}}{\partial y} + \frac{2i\alpha}{c^2} \left(\frac{v_{11}}{-i\alpha}\right)^2 (2+c) - i\alpha u_{11}^2 .$$

Use the continuity equation,

$$\frac{\partial v_{22}}{\partial y} = -2i\alpha u_{22} ,$$

to eliminate  $u_{22}$  :

$$\begin{aligned}\frac{Re}{\kappa} \left[ c \frac{\partial^3}{\partial y^3} \left(\frac{v_{22}}{-2i\alpha}\right) + 8\alpha^2 \left(\frac{v_{22}}{-2i\alpha}\right) + \alpha(4\alpha - ic Re) \left(\frac{v_{11}}{-i\alpha}\right) \frac{\partial u_{11}}{\partial y} \right. \\ \left. + 2\alpha \left(\frac{2\alpha}{c^2} (2+c) - i Re\right) \left(\frac{v_{11}}{-i\alpha}\right)^2 \right] + 2i\alpha \left[ \left(\frac{v_{22}}{-2i\alpha}\right) - \frac{1}{c^2} \left(\frac{v_{11}}{-i\alpha}\right)^2 \right] = 0 .\end{aligned}$$

Substituting

$$u_{22} = A^2 \frac{\partial \psi_2}{\partial y} \quad v_{22} = -2i\alpha\psi_2 \quad u_{11} = A \frac{\partial \psi}{\partial y} \quad v_{11} = -i\alpha\psi$$

into this relation gives

$$\begin{aligned} \frac{Re}{\kappa} \left[ c \frac{\partial^3 \psi_2}{\partial y^3} + 8\alpha^2 \psi_2 + \alpha(4\alpha - ic Re) \psi \frac{\partial^2 \psi}{\partial y^2} - 2\alpha \left( 2\alpha \frac{2+c}{c^2} - i Re \right) \psi^2 \right] \\ + 2i\alpha \left[ \psi_2 - \left( \frac{\psi}{c} \right)^2 \right] = 0 \\ c \frac{\partial \psi_2}{\partial y} + 2\psi_2 + \psi \frac{\partial^2 \psi}{\partial y^2} - \frac{2+c}{c} \psi^2 = 0 . \end{aligned}$$

The boundary conditions at  $y = +1$  and equation 3.3 require that  $\psi_2(y)$  be an odd function about  $y = 0$ .

From the coefficient of  $\epsilon E$  I obtain

$$\begin{aligned} -i\alpha c \eta_{12} - c_g \frac{\partial \eta_{11}}{\partial \xi} &= v_{12} \\ 0 &= u_{12} + 2\eta_{12} \\ P_{12}^{(1)} &= -\frac{\kappa}{Re^2} \left( i\alpha \eta_{12} + \frac{\partial \eta_{11}}{\partial \xi} \right) , \end{aligned}$$

and, eliminating  $\eta_{12}$  and  $\eta_{11}$ ,

$$i\alpha c u_{12} - 2v_{12} - 2\frac{c_g}{c} \frac{\partial}{\partial \xi} \left( \frac{v_{11}}{-i\alpha} \right) = 0 \quad P_{12}^{(1)} = \frac{\kappa}{c Re^2} \left[ v_{12} - \frac{c - c_g}{c} \frac{\partial}{\partial \xi} \left( \frac{v_{11}}{-i\alpha} \right) \right] .$$

The continuity equation and  $x$ -momentum equation hold throughout the fluid, and, evaluating these equations at the lower wall to obtain

$$u_{12} = \frac{\partial}{\partial y} \left( \frac{v_{12}}{-i\alpha} \right) - \frac{1}{i\alpha} \frac{\partial u_{11}}{\partial \xi} , \quad P_{12}^{(1)} = \frac{1}{Re} \left( \frac{\partial^2 u_{12}}{\partial y^2} - \alpha^2 u_{12} + 2i\alpha \frac{\partial u_{11}}{\partial \xi} \right) ,$$

I can eliminate the variables  $u_{11}$ ,  $u_{12}$ , and  $P_{12}^{(1)}$  to find

$$\begin{aligned} c \frac{\partial v_{12}}{\partial y} + 2v_{12} - 2\frac{c - c_g}{c} \frac{\partial}{\partial \xi} \left( \frac{v_{12}}{-i\alpha} \right) &= 0 \\ \frac{Re}{\kappa} \left[ c \frac{\partial^3 v_{12}}{\partial y^3} + 2\alpha^2 v_{12} - 2\frac{\partial}{\partial \xi} \left( \frac{v_{12}}{-i\alpha} \right) - 2\alpha^2 \frac{2c - c_g}{c} \frac{\partial}{\partial \xi} \left( \frac{v_{12}}{-i\alpha} \right) \right] \\ - i\alpha \left[ v_{12} - \frac{c - c_g}{c} \frac{\partial}{\partial \xi} \left( \frac{v_{12}}{-i\alpha} \right) \right] &= 0 . \end{aligned}$$

Substituting

$$u_{12} = \frac{1}{i} \frac{\partial A}{\partial \xi} \frac{\partial \psi_{10}}{\partial y} \quad v_{12} = -\frac{\partial A}{\partial \xi} (\alpha \psi_{10} + \psi) \quad u_{11} = \frac{\partial \psi}{\partial y} \quad v_{11} = -i\alpha \psi ,$$

eliminating  $\partial^3 \psi / \partial y^3$  , and factoring out  $\partial A / \partial \xi$  gives

$$\begin{aligned} c \frac{\partial \psi_{10}}{\partial y} + 2\psi_{10} + 2 \frac{c - c_g}{\alpha c} \psi &= 0 \\ \frac{Re}{\kappa} \left[ c \frac{\partial^3 \psi_{10}}{\partial y^3} + 2\alpha^2 \psi_{10} + 2\alpha \frac{3c - c_g}{c} \psi \right] \\ + i\alpha \left[ \psi_{10} + \frac{2c - c_g}{\alpha c} \psi \right] &= 0 . \end{aligned} \quad (3.7)$$

From the coefficient of  $\epsilon^{3/2} E$  I obtain

$$\begin{aligned} -i\alpha c \eta_{13} - c_g \frac{\partial \eta_{11}}{\partial \xi} + \frac{\partial \eta}{\partial \tau} &= v_{13} + \eta_{22} \frac{\partial \bar{v}_{11}}{\partial y} + \bar{\eta}_{11} \frac{\partial v_{22}}{\partial y} + \eta_{11} \bar{\eta}_{11} \frac{\partial^2 v_{11}}{\partial y^2} + \frac{\eta_{11}^2}{2} \frac{\partial^2 \bar{v}_{11}}{\partial y^2} \\ 0 = u_{13} + 2\eta_{13} \\ + \eta_{11} \frac{\partial u_{20}}{\partial y} + \eta_{22} + \eta_{22} \frac{\partial \bar{u}_{11}}{\partial y} + \bar{\eta}_{11} \frac{\partial u_{22}}{\partial y} - 2\bar{\eta}_{11} \eta_{22} + \eta_{11} \bar{\eta}_{11} \frac{\partial^2 u_{11}}{\partial y^2} + \eta_{11}^2 \frac{\partial^2 \bar{u}_{11}}{\partial y^2} \\ P_{13}^{(1)} &= -\frac{\kappa}{Re^2} \left( i\alpha \eta_{13} + \frac{\partial \eta_{12}}{\partial \xi} \right) , \end{aligned}$$

and, eliminating  $\eta_{13}$  ,

$$\begin{aligned} 0 = i\alpha c u_{13} - 2v_{13} + 2c_g \frac{\partial \eta_{12}}{\partial \xi} - 2 \frac{\partial \eta_{11}}{\partial \tau} - 2i\alpha c \bar{\eta}_{11} \eta_{22} + i\alpha c \eta_{11} \frac{\partial u_{20}}{\partial y} \\ + \eta_{22} \left( i\alpha c \frac{\partial \bar{u}_{11}}{\partial y} + 2 \frac{\partial \bar{v}_{11}}{\partial y} \right) + \bar{\eta}_{11} \left( i\alpha c \frac{\partial u_{22}}{\partial y} + 2 \frac{\partial v_{22}}{\partial y} \right) \\ + \eta_{11} \bar{\eta}_{11} \left( i\alpha c \frac{\partial^2 u_{11}}{\partial y^2} + 2 \frac{\partial^2 v_{11}}{\partial y^2} \right) + \frac{\eta_{11}^2}{2} \left( i\alpha c \frac{\partial^2 \bar{u}_{11}}{\partial y^2} \right) \\ P_{13}^{(1)} &= \frac{\kappa}{c Re^2} \left[ v_{13} - (c - c_g) \frac{\partial \eta}{\partial \xi} - \frac{\partial \eta}{\partial \tau} \right. \\ &\quad \left. + \eta_{22} \frac{\partial \bar{v}_{11}}{\partial y} + \bar{\eta}_{11} \frac{\partial v_{22}}{\partial y} + \eta_{11} \bar{\eta}_{11} \frac{\partial^2 v_{11}}{\partial y^2} + \frac{\eta_{11}^2}{2} \frac{\partial^2 \bar{v}_{11}}{\partial y^2} \right] . \end{aligned}$$

The continuity and  $x$ -momentum equation hold throughout the fluid, and, evaluating these equations at the lower wall,

$$\begin{aligned}
u_{13} &= \frac{i}{\alpha} \frac{\partial v_{13}}{\partial y} - \frac{1}{\alpha^2} \frac{\partial^2 v_{12}}{\partial \xi \partial y} - \frac{i}{\alpha^3} \frac{\partial^3 v_{11}}{\partial \xi^2 \partial y}, \\
&- i\alpha c u_{13} + 2v_{13} + P_{13}^{(1)} - c_g \frac{\partial u_{12}}{\partial \xi} + \frac{\partial u_{11}}{\partial \tau} + i\alpha u_{20} u_{11} + v_{11} \frac{\partial u_{20}}{\partial y} \\
&+ v_{22} \frac{\partial \bar{u}_{11}}{\partial y} + i\alpha u_{22} \bar{u}_{11} + \bar{v}_{11} \frac{\partial u_{22}}{\partial y} = \frac{1}{Re} \left( \frac{\partial^2 u_{13}}{\partial y^2} - \alpha^2 u_{13} + 2i\alpha \frac{\partial u_{12}}{\partial \xi} + \frac{\partial^2 u_{11}}{\partial \xi^2} \right).
\end{aligned}$$

I can eliminate the variables  $u_{11}$ ,  $u_{12}$ ,  $u_{13}$ ,  $\eta_{11}$ ,  $\eta_{12}$ ,  $\eta_{13}$ ,  $u_{20}$ , and  $P_{12}^{(1)}$  to find

$$\begin{aligned}
c \frac{\partial v_{13}}{\partial y} + 2v_{13} &= -\frac{2}{c} \frac{\partial A}{\partial \tau} + i\alpha Re P_{20}^{(1)} \psi A + i\alpha \left(F + \frac{2}{c}G\right) A|A|^2 + \frac{2i(c - c_g)}{c} K \frac{\partial^2 A}{\partial \xi^2} \\
\frac{Re}{\kappa} \left[ c \frac{\partial^3 v_{11}}{\partial y^3} - 2\alpha^2 v_{13} \right] - i\alpha v_{13} &= \frac{i\alpha}{c} \left( \frac{2i\alpha Re}{\kappa} - 1 \right) \psi \frac{\partial A}{\partial \tau} + (i\alpha Re P_{20}^{(1)} \psi) \frac{\alpha^2 Re}{\kappa} A \\
&+ \alpha^2 \left[ \frac{c Re^2}{\kappa} \left( \frac{i\alpha}{c Re} - 1 \right) \left( F + \frac{2}{c}G \right) + \frac{c Re^2}{\kappa} H - \frac{G}{c} \right] A|A|^2 \\
&- \left[ \frac{\alpha}{c} (2c - c_g) K + \psi - \frac{2i\alpha Re}{\kappa} \left[ \frac{\alpha}{c} (3c - c_g) K + i c_g Re K + 3\psi \right] \right] \frac{\partial^2 A}{\partial \xi^2}
\end{aligned}$$

where

$$\begin{aligned}
F &\equiv \left( \psi_2 - \frac{\psi^2}{c^2} \right) \left( \frac{\partial^2 \bar{\psi}}{\partial y^2} - 2\frac{\bar{\psi}}{c} \right) + \bar{\psi} \frac{\partial^2 \psi_2}{\partial y^2} + \frac{\psi \bar{\psi}}{c} \frac{\partial^3 \psi}{\partial y^3} + \frac{\psi^2}{2c} \frac{\partial^3 \bar{\psi}}{\partial y^3} \\
G &\equiv \left( \psi_2 - \frac{\psi^2}{c^2} \right) \frac{\partial \bar{\psi}}{\partial y} - 2\bar{\psi} \frac{\partial \psi_2}{\partial y} - \frac{\psi \bar{\psi}}{c} \frac{\partial^2 \psi}{\partial y^2} + \frac{\psi^2}{2c} \frac{\partial^2 \bar{\psi}}{\partial y^2} \\
H &\equiv \frac{\partial \psi}{\partial y} S(-1) + \frac{\partial \bar{\psi}}{\partial y} \frac{\partial \psi_2}{\partial y} + \bar{\psi} \frac{\partial^2 \psi_2}{\partial y^2} - 2\psi_2 \frac{\partial^2 \psi}{\partial y^2} \\
K &\equiv \psi_{10} + \frac{c - c_g}{\alpha c} \psi
\end{aligned}$$

all evaluated at  $y = -1$ .

Define a new function

$$\hat{v}_{13} = v_{13} - (1 - y^2 - c) r_2 + r_0$$

where the constants  $r_2$  and  $r_0$  are chosen so that

$$\begin{aligned}
0 = c \frac{\partial \hat{v}_{13}}{\partial y} - 2\hat{v}_{13} & \quad 0 = i\alpha \hat{v}_{13} + \frac{Re}{\kappa} \left( 2\alpha^2 \hat{v}_{13} - c \frac{\partial^3 \hat{v}_{13}}{\partial y^3} \right) & \text{at } y = +1 \\
0 = c \frac{\partial \hat{v}_{13}}{\partial y} + 2\hat{v}_{13} & \quad 0 = i\alpha \hat{v}_{13} + \frac{Re}{\kappa} \left( 2\alpha^2 \hat{v}_{13} + c \frac{\partial^3 \hat{v}_{13}}{\partial y^3} \right) & \text{at } y = -1.
\end{aligned}$$

Since  $\hat{v}_{13}$  and the Orr-Sommerfeld eigenfunction  $\psi$  have the same boundary conditions, if  $\Phi$  is the adjoint to  $\psi$ , then

$$\int_{-1}^{+1} \Phi \mathcal{L} \hat{v}_{13} dy = 0 .$$

From the above definition I find that

$$\begin{aligned} \mathcal{L} \hat{v}_{13} &\equiv \mathcal{L} v_{13} + \mathcal{F}(r_2, r_0) \\ &= \mathcal{L} v_{13} + \alpha^2(1 - y^2 - c)^2 r_2 - \alpha^2(1 - y^2 - c) r_0 + 2 r_0 \\ &\quad - \frac{i\alpha}{Re} [4r_2 + \alpha^2(1 - y^2 - c)r_2 - \alpha^2 r_0] , \end{aligned}$$

where  $\mathcal{F}$  is a function of  $y$ . Multiplying the right-hand side by  $\Phi$  and, taking advantage of the symmetry, integrating from zero to one gives

$$0 = \theta_1 \frac{\partial A}{\partial \tau} - \theta_2 \frac{\partial^2 A}{\partial \xi^2} - \hat{P} \theta_3 A - \theta_4 A |A|^2 , \quad (3.8)$$

where

$$\begin{aligned} \theta_1 &= \int_0^1 \Phi \left\{ (D^2 - \alpha^2) \psi(y) - \frac{\psi(1)}{c} [2 - \alpha^2(1 - y^2 - c) + \frac{i\alpha^3}{Re}] \right\} dy \\ \theta_2 &= i \int_0^1 \Phi \left\{ (1 - y^2 - c_g - \frac{4i\alpha}{Re})(D^2 - \alpha^2)(\psi_{10} + \frac{\psi}{\alpha}) - 2\alpha^2(1 - y^2 - c)(\psi_{10} + \frac{\psi}{\alpha}) \right. \\ &\quad \left. + 2(\psi_{10} + \frac{\psi}{\alpha}) - [(c - c_g - \frac{2i\alpha}{Re})(D^2 + \alpha^2)\frac{\psi}{\alpha} + (1 - y^2 - c)D^2\frac{\psi}{\alpha} + 2\frac{\psi}{\alpha}] + \mathcal{F}(r_1, r_0) \right\} dy \\ r_1 &\equiv \left\{ K + \frac{\psi(1)}{\alpha} + \frac{2}{\kappa} \left( \frac{2\alpha K + 3\psi(1)}{i Re} + c_g K \right) \right\} / c \left( \frac{2i\alpha Re}{\kappa} - 1 \right) \\ r_0 &\equiv \frac{c - c_g}{c} K \quad K \equiv \psi_{10}(1) + \frac{c - c_g}{\alpha c} \psi(1) \\ \theta_3 &= -\frac{3}{2} i \alpha \int_0^1 \Phi \left\{ (1 - y^2)(D^2 - \alpha^2) \psi + 2\psi + \mathcal{F}(r_3, r_2) \right\} dy \\ r_3 &\equiv \psi(1) / c \left( \frac{2i\alpha Re}{\kappa} - 1 \right) \quad r_2 \equiv \psi(1) \\ \theta_4 &= i \alpha \int_0^1 \Phi \left\{ \frac{\partial \psi_2}{\partial y} (D^2 - \alpha^2) \bar{\psi} + 2\psi_2 (D^2 - \alpha^2) \frac{\partial \bar{\psi}}{\partial y} - 2 \frac{\partial \bar{\psi}}{\partial y} (D^2 - 4\alpha^2) \psi_2 \right. \\ &\quad \left. - \bar{\psi} (D^2 - 4\alpha^2) \frac{\partial \psi_2}{\partial y} - [S(y) - \frac{3}{2} S_0(1 - y^2)] (D^2 - \alpha^2) \psi + \psi \left( \frac{\partial^2 S}{\partial y^2} + 3S_0 \right) \right\} dy \end{aligned}$$

$$-\frac{1}{2}\mathcal{F}(r_5, r_4)\}dy \quad r_4 \equiv F + \frac{2}{c}G + 3\psi(1)S_0$$

$$r_5 \equiv \left\{\frac{2c}{\kappa}\left(F + \frac{2}{c}G + H\right) + F + 3S_0\psi(1)\right\}/c\left(\frac{2i\alpha Re}{\kappa} - 1\right)$$

and the constants  $F$ ,  $G$ , and  $H$  are now evaluated at  $y = +1$  and given by

$$F \equiv \left(\psi_2 + \frac{\psi^2}{c^2}\right)\left(\frac{\partial^2\bar{\psi}}{\partial y^2} - 2\frac{\bar{\psi}}{c}\right) + \bar{\psi}\frac{\partial^2\psi_2}{\partial y^2} + \frac{\psi\bar{\psi}}{c}\frac{\partial^3\psi}{\partial y^3} + \frac{\psi^2}{2c}\frac{\partial^3\bar{\psi}}{\partial y^3}$$

$$G \equiv \left(\psi_2 + \frac{\psi^2}{c^2}\right)\frac{\partial\bar{\psi}}{\partial y} - 2\bar{\psi}\frac{\partial\psi_2}{\partial y} - \frac{\psi\bar{\psi}}{c}\frac{\partial^2\psi}{\partial y^2} + \frac{\psi^2}{2c}\frac{\partial^2\bar{\psi}}{\partial y^2}$$

$$H \equiv \frac{\partial\psi}{\partial y}S(+1) + \frac{\partial\bar{\psi}}{\partial y}\frac{\partial\psi_2}{\partial y} + \bar{\psi}\frac{\partial^2\psi_2}{\partial y^2} - 2\psi_2\frac{\partial^2\psi}{\partial y^2}$$

$$K \equiv \psi_{10} + \frac{c - c_g}{\alpha c}\psi$$

The Landau equation for  $|A|^2$  is found by assuming  $A$  is a function of  $\tau$  only and adding  $\bar{A}$  times equation 3.8 with  $A$  times the complex conjugate of equation 3.8 to obtain

$$\frac{\partial|A|^2}{\partial\tau} = \hat{P}\left(\frac{\theta_3}{\theta_1} + \frac{\bar{\theta}_3}{\bar{\theta}_1}\right)|A|^2 + \left(\frac{\theta_4}{\theta_1} + \frac{\bar{\theta}_4}{\bar{\theta}_1}\right)|A|^4.$$

Consider the equation for the mean-flow (or time averaged) pressure gradient,

$$P_0^{(1)} = U\left[-2/Re + \epsilon P_{20}^{(1)} + O(\epsilon^{3/2})\right]$$

$$= U\left[-2/Re + \epsilon\left\{\frac{3}{2}\hat{P}(1-y^2) + |A|^2\left[S(y) - \frac{3}{2}S_0(1-y^2)\right]\right\} + O(\epsilon^{3/2})\right],$$

the time averaged fluid flux,

$$Q = \int_{-1}^{+1} u_0 dy = \frac{4U}{3} + \epsilon 2U\hat{P} + O(\epsilon^{3/2}),$$

and the Landau equation. A constant solution of this equation,

$$|A|^2 = -\hat{P}\left(\frac{\theta_3}{\theta_1} + \frac{\bar{\theta}_3}{\bar{\theta}_1}\right)/\left(\frac{\theta_4}{\theta_1} + \frac{\bar{\theta}_4}{\bar{\theta}_1}\right),$$

shown in Figure 3.2 bifurcates at  $\epsilon = 0$  from plane Poiseuille flow at  $Q = 4U/3$ , and the parameter  $\hat{P}$  is seen as a measure of the amplitude of  $A$ . However, since  $\epsilon\hat{P}$

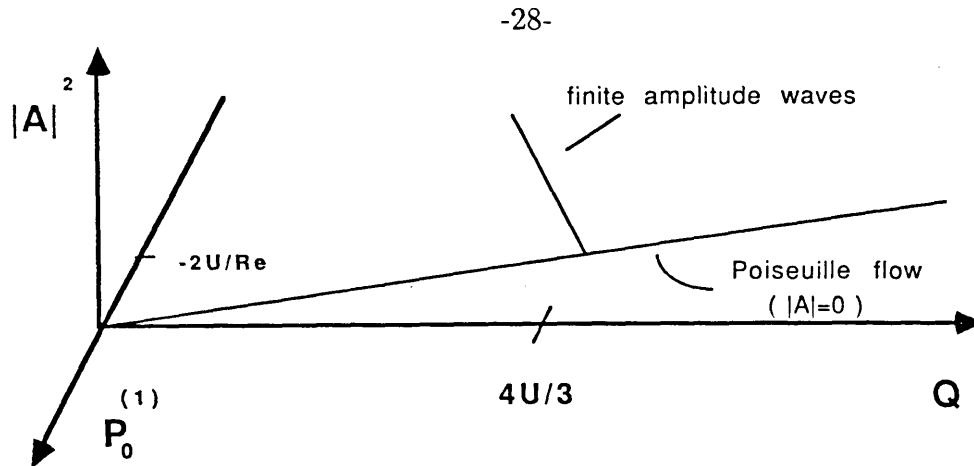


Figure 3.2: Configuration space for two-dimensional finite amplitude waves in Poiseuille flow.

also measures the change in the flux and the change in the mean pressure gradient (even when  $|A|^2 = 0$ ),  $\hat{P}$  can also be interpreted as the change in the Reynolds number. As shown in Figure 3.2, this weakly nonlinear formalism gives the linear approximation of the bifurcation to finite amplitude disturbances of Poiseuille flow (Landman, [1987]), and the actual value of  $\hat{P}$  chosen is unimportant. What is important is whether the bifurcation is supercritical (*i.e.*  $|A|^2 > 0$  for  $Re > Re_{critical}$ ) or subcritical. A subcritical bifurcation is shown in Figure 3.2 since this is what occurs for rigid wall Poiseuille flow. From the Landau equation it is easily seen that for a supercritical bifurcation the solution  $|A|^2$  is stable with respect to spatially homogeneous ( $\partial^2 A / \partial \xi^2 = 0$ ) disturbances and that for a subcritical bifurcation the solution is unstable to these disturbances. For consistency with Stewartson and Stuart [1971] I will let  $\hat{P} = 2/3 Re$ .

### 3.3 Numerical Results

The values of the Ginzburg-Landau coefficients must be calculated numerically. Using an initial guess for  $\psi$ ,  $\Phi$ ,  $\psi_{10}$ , and  $\psi_2$  for  $Re \ll 1$  (Drazin and Reid, [1981]), I continued the solution branch using the program AUTO developed by Doedel and

|                 | Davey, et.al.          | 89 grid points           | 101 grid points          |
|-----------------|------------------------|--------------------------|--------------------------|
| $\alpha_c$      | 1.02055                | 1.020547                 | 1.020547                 |
| $Re_c$          | 5772.22                | 5772.2218                | 5772.2218                |
| $c_{cr}$        | 0.264                  | 0.264000                 | 0.264000                 |
| $c_{ci}$        | 0.                     | 0.                       | 0.                       |
| $c_g$           | 0.383                  | 0.3831                   | 0.3831                   |
| $S_0$           | -87.2                  | -87.067                  | -87.067                  |
| real $\theta_1$ | 1.                     | 1.                       | 1.                       |
| imag $\theta_1$ | 0.                     | $< 10^{-16}$             | $< 10^{-16}$             |
| real $\theta_2$ | 0.187                  | 0.1867                   | 0.1867                   |
| imag $\theta_2$ | 0.0275                 | 0.02748                  | 0.02748                  |
| real $\theta_3$ | $0.168 \times 10^{-5}$ | $0.16825 \times 10^{-5}$ | $0.16825 \times 10^{-5}$ |
| imag $\theta_3$ | $0.811 \times 10^{-5}$ | $0.81128 \times 10^{-5}$ | $0.81128 \times 10^{-5}$ |
| real $\theta_4$ | 30.8                   | 30.95616                 | 30.95619                 |
| imag $\theta_4$ | -173                   | -172.83343               | -172.83342               |

Table 3.1: The Ginzburg-Landau coefficients for rigid walls.

Kernevez [1985] to  $Re_c = 5772$ . The integrals for  $\theta_1$ ,  $\theta_2$ ,  $\theta_3$ , and  $\theta_4$  are performed in AUTO using a composite Gaussian quadrature formula for Lagrange basis polynomials. The coefficients calculated at  $Re_c$  agree very well with those calculated by Davey, Hocking, and Stewartson [1974] for rigid walls (Table 3.1).

Since from equation 2.1

$$\delta \tilde{p}_W = -\tilde{\kappa} \tilde{\eta},$$

I will identify the limit of  $\tilde{\kappa} \rightarrow \infty$  (and since  $\kappa = \tilde{\kappa} L^3 \rho / \mu^2$ ,  $\kappa \rightarrow \infty$  as well) as the rigid wall limit and can use the solution for rigid walls as an initial guess for the finite

| $\kappa$           | $Re_c$   | real part of $\theta_4/\theta_1$ |
|--------------------|----------|----------------------------------|
| rigid              | 5772.22  | 30.956                           |
| $1000 \times 10^7$ | 5774.38  | 30.827                           |
| $100 \times 10^7$  | 5793.95  | 29.690                           |
| $10 \times 10^7$   | 6002.49  | 20.102                           |
| $5 \times 10^7$    | 6266.02  | 12.593                           |
| $3 \times 10^7$    | 6685.39  | 6.247                            |
| $1.5 \times 10^7$  | 8371.04  | 0.200                            |
| $1.4 \times 10^7$  | 8757.69  | -0.082                           |
| $1.3 \times 10^7$  | 9296.14  | -0.311                           |
| $1.2 \times 10^7$  | 10118.25 | -0.473                           |
| $1.1 \times 10^7$  | 11646.88 | -0.532                           |

Table 3.2: The effect of compliant walls on stability.

$\kappa$  branch at  $\kappa = 1.0 \times 10^{10}$ . Once on this solution branch I continued in decreasing  $\kappa$  as shown in Table 3.2. For the Orr-Sommerfeld eigenfunction,  $\psi$ , the boundary condition

$$i\alpha\psi + \frac{Re}{\kappa}(2\alpha^2\psi - c\frac{\partial^3\psi}{\partial y^3}) = 0$$

must hold at the upper wall. For rigid walls

$$\frac{\partial^3\psi}{\partial y^3} \simeq i 3000$$

at the upper wall, so an estimate of the value of  $\kappa$  for which

$$\psi(+1) \simeq \frac{c Re}{i\alpha\kappa} \frac{\partial^3\psi}{\partial y^3} \sim 1$$

is  $\kappa \sim 10^7$ , and it is no surprise that the Ginzburg-Landau constants begin to deviate significantly from the rigid wall values for  $\kappa \sim 10^8$ .

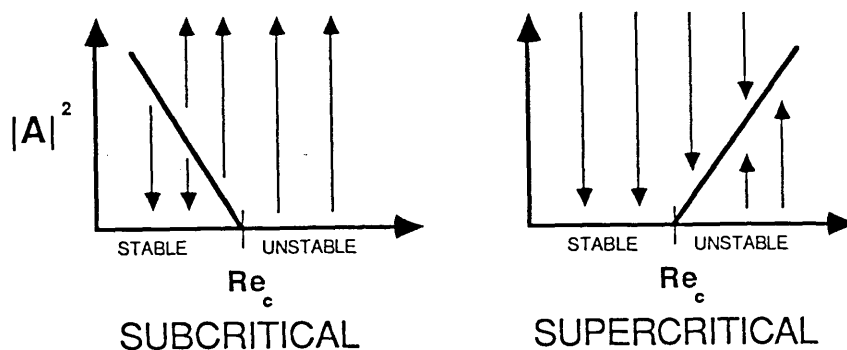


Figure 3.3: Subcritical and supercritical bifurcations from zero amplitude.

The eigenvalues of the eigenfunction and its adjoint form a complex conjugate pair, but numerically each is calculated independently, and these calculations provide a test for numerical accuracy. In all my calculations these eigenvalues differed by less than one part in  $10^{10}$ . Another numerical test is the value of the imaginary part of  $c_g$ , which should be zero at  $Re = Re_c$  (Stewartson and Stuart, [1971]). For single precision calculations on a Cray XM/P the ratio of the imaginary part to the real part of  $c_g$  was  $10^{-5}$ , and for double precision calculations on a Sun 3/260 the ratio was  $10^{-7}$ .

As Benjamin showed [1960,1964], the critical Reynolds number grows as  $\kappa$  decreases, but for the range I have considered its value has less than doubled. The real part of  $\theta_4/\theta_1$  has decreased monotonically from its rigid wall value of 30.956 to a value of  $-0.532$  at  $\kappa = 1.1 \times 10^7$ , and the bifurcation to finite amplitude disturbances has gone from subcritical to supercritical (Figure 3.3). Although this weakly nonlinear formalism is only valid in the limit of small amplitude, there must be a range of amplitude where the nonlinear wave is stable. I will discuss the implications of this result in Chapter 5.

| $\kappa$        | damping coefficient | $Re_c$  | real part of $\theta_4/\theta_1$ |
|-----------------|---------------------|---------|----------------------------------|
| $3 \times 10^7$ | 0                   | 6685.39 | 6.247                            |
| $3 \times 10^7$ | $1 \times 10^6$     | 6475.32 | 7.487                            |
| $3 \times 10^7$ | $2 \times 10^6$     | 6290.51 | 8.703                            |

Table 3.3: The effect of damping on stability.

To get an intuitive idea of how flexible the wall must be at  $\kappa = 1.1 \times 10^7$ , consider the experimental result for rigid wall boundary layer flow that three-dimensional perturbations grow rapidly once the Tollmien-Schlichting waves reach a threshold amplitude of about 1% of the free stream velocity (Bayly, *et al.*, [1988]). If I take this amplitude as an upper limit for a small two-dimensional disturbance and let  $\delta p_W$  be 0.01 and  $\kappa/Re^2$  to be 0.1 ( $\kappa = 1.1 \times 10^7$  in Table 3.2), then  $\eta$  must be 0.1 or about 5% of the channel width.

If I make the substitution

$$\kappa \longrightarrow \kappa - i\alpha c d$$

in the boundary condition at the upper wall, I include the nondimensional damping coefficient in the wall model. The results of these calculations are shown in Table 3.3 for the value of  $\kappa = 3 \times 10^7$ . The decrease in the critical Reynolds number was interpreted by Benjamin as evidence that damping destabilizes the flow. Since the energy supply to a neutral wave on the boundary balances the rate of energy absorption, he argued that the Reynolds number has to be reduced in order to make the relative viscous dissipation sufficient to restore the energy balance. I have found that, in addition to the decrease of  $Re_c$ , damping also causes the real part of  $\theta_4/\theta_1$  to grow larger. Because the finite amplitude disturbance is stable when the real part of  $\theta_4/\theta_1$  is less than zero, the effect of damping in the weakly nonlinear formalism is

destabilizing as well.

# Chapter 4

## Quasisteady solutions

In this chapter I will discuss the quasisteady solutions of the Ginzburg-Landau equation for compliant walls using the formalism of Landman [1987]. For rigid walls, the spatial variation of these solutions may be periodic, quasiperiodic, or chaotic. I have found that although the periodic and quasiperiodic solutions persist at  $\kappa = 1.1 \times 10^7$ , the chaotic solutions do not.

The quasisteady solutions of the normal form of the Ginzburg-Landau equation,

$$\frac{\partial A}{\partial \tau} = (a_r + ia_i) \frac{\partial^2 A}{\partial x^2} + \sigma_r A + (d_r + id_i) A |A|^2 ,$$

are of the form

$$A(x, \tau) = e^{-i\Omega\tau} \Phi(x - c\tau) ,$$

where the wavespeed  $c$  provides an order  $\epsilon^{1/2}$  correction to the group velocity,  $c_g + \epsilon^{1/2}c$ . This  $c$  should not be confused with the eigenvalue of the Orr-Sommerfeld equation, which is fixed at  $c_{rc}$ . The values of the Ginzburg-Landau coefficients are given in Table 4.1. The numerical value of  $a_r$  is +1 for the wall models I have studied. Substituting into the Ginzburg-Landau equation gives an ordinary differential equation for  $\Phi(X)$  :

$$(a_r + ia_i)\Phi'' + c\Phi' + (\sigma_r + i\Omega)\Phi + (d_r + id_i)\Phi|\Phi|^2 = 0 ,$$

where  $X \equiv x - c\tau$ . Following Landman I rewrite this equation as

$$\Phi'' + c_1(1 - ia_0)\Phi' + (\delta_1 + i\beta)\Phi = (\delta_2 + i\gamma)\Phi|\Phi|^2$$

where

$$\beta \equiv (a_r\Omega - a_i\sigma_r)/|a|^2 , \quad \gamma \equiv (a_id_r - a_r d_i)/|a|^2 ,$$

| $\kappa$          | $a_r$ | $a_i$  | $d_r$ | $d_i$  |
|-------------------|-------|--------|-------|--------|
| rigid             | 1     | 0.1472 | 1     | -5.583 |
| $1.1 \times 10^7$ | 1     | -4.574 | -1    | -63.87 |

Table 4.1: The coefficients for the normal form of the Ginzburg-Landau equation for rigid and compliant walls.

$$\begin{aligned} \delta_1 &\equiv (a_r \sigma_r + a_i \Omega) / |a|^2, & \delta_2 &\equiv (-a_r d_r - a_i d_i) / |a|^2, \\ c_1 &\equiv c a_r / |a|^2, & a_0 &\equiv a_i / |a|^2. \end{aligned}$$

The coefficients  $\gamma$ ,  $\delta_2$ , and  $a_0$  are determined by the Ginzburg-Landau coefficients, and  $\beta$ ,  $\delta_1$ , and  $c_1$  depend linearly on the two undetermined parameters  $\Omega$  and  $c$ , the temporal frequency of oscillation and the group velocity correction.

This second order complex ordinary differential equation can be written as a first order system in four real variables, but because of the phase invariance of the Ginzburg-Landau equation this system possesses a rotational symmetry. Following Sirovich and Newton [1986], I remove this apparent degree of freedom by defining the variables  $r$ ,  $s$ , and  $w$  where

$$\Phi = r^{1/2} \exp\left[i \int^X s dX\right], \quad w = \frac{r'}{2r}.$$

The system of first order ordinary differential equations is given by

$$\begin{aligned} r' &= 2 w r, \\ s' &= -\beta + \gamma r - 2 s w - c_1 (s - a_0 w), \\ w' &= -\delta_1 + \delta_2 r + s^2 - w^2 - c_1 (a_0 s + w). \end{aligned}$$

The reflectional symmetry of the Ginzburg-Landau equation (where the equation remains invariant under the transformation  $x \rightarrow -x$ ) appears in this 3D system

under the transformation

$$X \rightarrow -X, \quad c \rightarrow -c, \quad (r, s, w) \rightarrow (r, -s, -w).$$

Furthermore, for a modified reduced system with coordinates  $(r^2, s, w)$  I find that

$$\frac{\partial(r^2)'}{\partial r^2} + \frac{\partial s'}{\partial s} + \frac{\partial w'}{\partial w} = -2c_1,$$

and the flow is converging for  $c > 0$ , diverging for  $c < 0$ , and volume preserving for  $c = 0$ . As noted by Landman, the phase contraction for  $c > 0$  does not imply that phase volumes remain bounded in a region of phase space, although solutions may approach an attracting set in phase space as  $X \rightarrow \infty$ .

There are four critical points for this 3D system called  $D_+$ ,  $D_-$ ,  $T_+$ , and  $T_-$  given by

$$D_{\pm} : \quad \begin{aligned} r_0 &= 0 \\ s_0 &= \frac{a_0 c_1}{2} \mp \operatorname{sgn}(\chi) \sqrt{\frac{|\zeta| + \xi}{2}} \\ w_0 &= \frac{-c_1}{2} \pm \sqrt{\frac{|\zeta| - \xi}{2}} \end{aligned}$$

where

$$\zeta = \xi + i\chi,$$

$$\xi(\Omega, c) = \delta_1 - \frac{1}{4}c_1^2(1 - a_0^2), \quad \chi(\Omega, c) = \beta + \frac{1}{2}a_0 c_1^2$$

$$T_{\pm} : \quad \begin{aligned} r_T &= \frac{\beta}{\gamma} + \frac{c_1^2 d_r}{2a_r \gamma^2} \pm \frac{c_1}{\gamma} \sqrt{\frac{c_1^2 d_r^2}{4a_r^2 \gamma^2} + \delta_1 - \frac{\delta_2 \beta}{\gamma}} \\ s_T &= \frac{c_1 d_r}{2a_r \gamma} \pm \sqrt{\frac{c_1^2 d_r^2}{4a_r^2 \gamma^2} + \delta_1 - \frac{\delta_2 \beta}{\gamma}} \\ w_T &= 0 \end{aligned}$$

The critical points  $D_{\pm}$  are zero amplitude solutions, while the  $T_{\pm}$  are the plane wave solutions

$$A = r_T^{1/2} e^{is_T X} e^{-i(\Omega + s_T c)t};$$

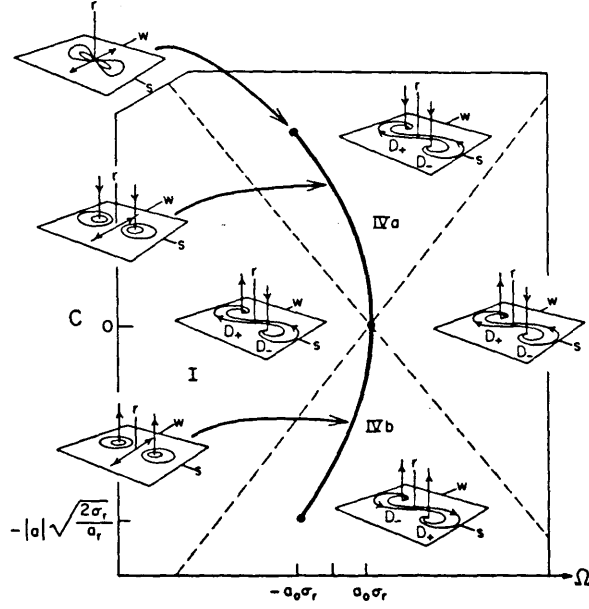


Figure 4.1: Phase portraits in the  $r = 0$  plane.

however, these solutions are only valid when  $r_T > 0$ . Since  $r = |A|^2$ , the critical points with  $r_T < 0$  are mathematical artifacts that are not solutions of the Ginzburg-Landau equation, and the plane  $r \equiv 0$  is an invariant subspace. The two lines in parameter space

$$\Omega = a_0 \sigma_r \pm \sqrt{\frac{\sigma_r}{a_r}} c, \quad \sigma_r > 0,$$

are the locations where each of the plane waves  $T_{\pm}$  bifurcates from zero amplitude (Landman, [1987]), and, although the  $r_T < 0$  critical points are artifacts, taking them into account at this bifurcation shows that this is a transcritical bifurcation (Guckenheimer and Holmes, [1983]).

In the plane  $r = 0$ , a branch cut in parameter space must be chosen in order to represent the critical points  $D_{\pm}$  continuously and unambiguously. The usual choice is to take  $\chi = 0$  when  $\xi \leq 0$ , and the branch cut corresponds to the parabolic

| Region     | Critical point stability                  |           |       |       |
|------------|---|-----------|-------|-------|
|            | Number of (negative,positive) eigenvalues |           |       |       |
|            | $T_+$                                     | $T_-$     | $D_+$ | $D_-$ |
| <b>I</b>   | -   | -         | (2,1) | (1,2) |
| <b>IIa</b> | (2,1)                                     | (3,0)     | (2,1) | (1,2) |
| <b>IIb</b> | (0,3)                                     | (1,2)     | (2,1) | (1,2) |
| <b>III</b> | (2,1)                                     | (1,2)     | (2,1) | (1,2) |
| <b>IVa</b> | (2,1)                                     | $r_T < 0$ | (3,0) | (1,2) |
| <b>IVb</b> | $r_T < 0$                                 | (1,2)     | (2,1) | (0,3) |
| <b>Va</b>  | (2,1)                                     | (3,0)     | (2,1) | (1,2) |
| <b>Vb</b>  | (0,3)                                     | (1,2)     | (2,1) | (1,2) |
| <b>VI</b>  | $r_T < 0$                                 | $r_T < 0$ | (2,1) | (1,2) |

Table 4.2: The numbers of stable and unstable eigenvalues of the critical points in the regions of  $\Omega - c$  parameter space.

segment

$$\Omega = a_0\sigma_r - \frac{a_i c^2}{2|a|^2} \quad , \quad \Omega \geq -a_0\sigma_r .$$

On crossing this cut by varying  $\Omega$  and  $c$  ,  $D_+$  and  $D_-$  swap identities. The eigenvalues of the critical points are given by

$$\lambda_1 = 2w_0 \quad , \quad \lambda_{2,3} = -(2w_0 + c_1) \pm i(2s_0 - a_0c_1) ,$$

and their phase portraits are shown in Figure 4.1 for rigid walls and  $\sigma_r = +1$  .

In discussing the stability of these critical points, I will mean the stability of the 3D system with respect to the variable  $X$  and not that of the Ginzburg-Landau equation as discussed in the previous chapter.

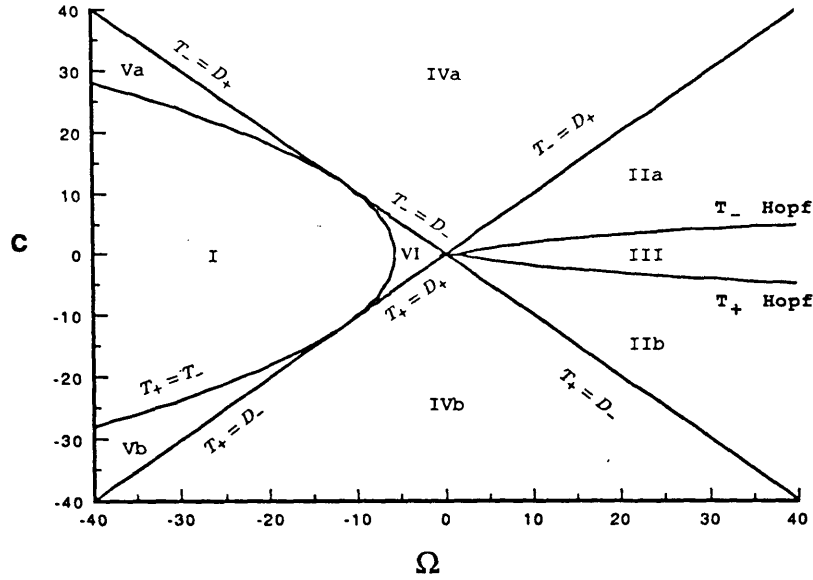


Figure 4.2: Stability diagram for rigid walls of the 3D system.

The characteristic equation of the linearization about the plane wave fixed points  $T_{\pm}$  is given by

$$\lambda^3 + 2 c_1 \lambda^2 + [c_1^2 + (2 s_T - a_0 c_1)^2 - 2 \delta_2 r_T] \lambda - 2 r_T [c_1 \delta_2 + \gamma (2 s_T - a_0 c_1)] = 0 . \quad (4.1)$$

Table 4.2 lists the number of negative and positive eigenvalues, or, more specifically, the number of eigenvalues with negative real parts and positive real parts, of each of the four critical points  $T_{\pm}$  and  $D_{\pm}$  in the different regions of parameter space. Figure 4.2 illustrates the location of these regions for rigid walls, while Figure 4.3 shows them for  $\kappa = 1.1 \times 10^7$  for  $\sigma_r = +1$ . As noted by Landman,  $|\sigma_r|$  can always be scaled to be 1, so these diagrams are representative of all supercritical Reynolds numbers. This table and figures were found by numerically calculating the eigenvalues and eigenvectors directly at the critical points at representative parameter values and studying the bifurcations numerically.

In addition to the transcritical bifurcation discussed above,  $T_{\pm}$  also coalesce in a saddle-node bifurcation along the parabola

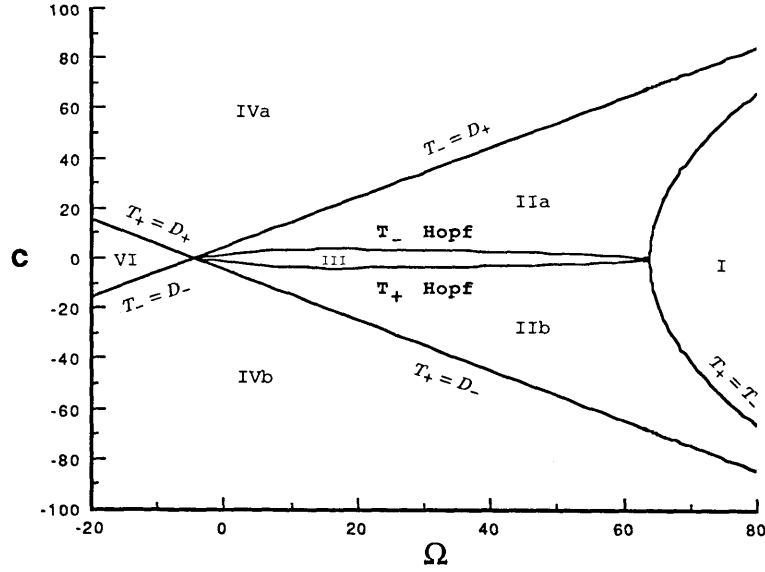


Figure 4.3: Stability diagram for  $\kappa = 1.1 \times 10^7$  of the 3D system.

$$\Omega = \sigma_r \frac{d_i}{d_r} - c^2 \left( \frac{d_r}{4(a_i d_r - a_r d_i)} \right) .$$

For rigid walls,  $T_{\pm}$  exists for

$$\Omega \geq \sigma_r \frac{d_i}{d_r} - c^2 \left( \frac{d_r}{4(a_i d_r - a_r d_i)} \right) ,$$

whereas for  $\kappa = 1.1 * 10^7$  (or any other value of  $\kappa$  where  $d_r = -1$ ) these critical points are found when

$$\Omega \leq \sigma_r \frac{d_i}{d_r} - c^2 \left( \frac{d_r}{4(a_i d_r - a_r d_i)} \right) .$$

Since

$$d_i/d_r = \frac{\text{imag part of } \theta_4/\theta_1}{\text{real part of } \theta_4/\theta_1} ,$$

the parabola is found further to the left in Figure 4.2 as  $\kappa$  becomes larger (and the real part of  $\theta_4/\theta_1$  approaches zero) until the real part of  $\theta_4/\theta_1$  changes sign, and the parabola is to the right of the line  $\Omega = a_i/a_r$  . A study of Figures 4.2 and 4.3 will show that the regions I, IV, and VI maintain their identity throughout this

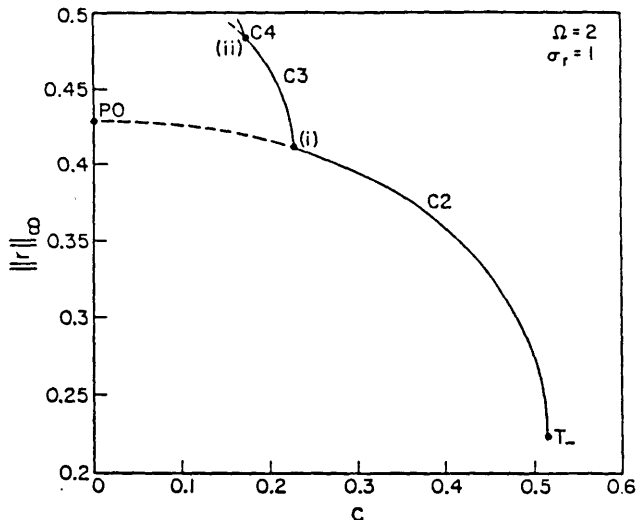


Figure 4.4: The continuation in  $c$  of the Hopf bifurcating branch from  $T_-$  into region III. Solid lines are stable periodic orbits. Supercritical period doubling bifurcations occur at (i) and (ii).

deformation although region V vanishes.

To find the Hopf bifurcations of  $T_{\pm}$ , I set  $\lambda = -\omega^2$  with  $\omega$  real in equation 4.1 and eliminate  $\omega$ ,  $s_T$ , and  $r_T$  to find

$$\begin{aligned}
 & c_1^2 [c_1^2 (1 + a_0^2) + 6\delta_1 - \beta(a_0 + 7\delta_2/\gamma)]^2 \\
 & + c_1^2 \frac{d_r}{\gamma a_r} [c_1^2(1 + a_0^2) + 6\delta_1 - \beta(a_0 + 7\delta_2/\gamma)][2\beta + c_1^2(a_0 - 7\delta_2/\gamma)] \\
 & - [\delta_1 - \delta_2\beta/\gamma][c_1^2(a_0 - 7\delta_2/\gamma) + 2\beta]^2 = 0 .
 \end{aligned}$$

This equation is cubic in  $\Omega$  and  $c_1^2$  (hence is symmetric with respect to  $c = 0$ ), and the curve crosses the line  $c = 0$  only at  $\Omega = a_i/a_r$  and  $\Omega = d_i/d_r$ . In Figures 4.2 and 4.3 the portions of the solution curve with  $r_T < 0$  are identical to values where  $\Omega < a_i/a_r$  and have been omitted. The actual calculation of these curves was done from the original 3D system by using the program AUTO to compute the two-parameter curve of Hopf bifurcation points. Landman [1987] has shown that the eigenvalue equation

governing the side-band instability of the Ginzburg-Landau equation (where the plane wave solutions are unstable to long wave modulations) is equivalent to the above equation for Hopf bifurcations in  $c - \Omega$  space.

In order to calculate the branch of periodic orbits that bifurcate from  $T_-$ , I set  $\Omega = 2$  and began the continuation at the boundary of regions IIa and III in parameter space. For rigid walls (Landman, [1987]) the branch undergoes at least two supercritical period doubling bifurcations (Figure 4.4) which may be the beginning of a period doubling cascade since at  $c = 0.14$  there exists a nonperiodic and possibly chaotic attractor. At  $\kappa = 1.1 \times 10^7$  the periodic orbits that bifurcate from this boundary remain stable down to  $c = 0$  in all cases I checked numerically. At  $c = 0$  the periodic orbit bifurcates to a (presumably stable) two-torus, and as  $c$  decreases the unstable periodic orbit shrinks and is finally absorbed by the critical point  $T_+$  at the boundary of regions III and IIb.

For rigid walls Landman found five families of heteroclinic and homoclinic connections for the 3D system as the parameters  $\Omega$  and  $c$  are varied. There are the homoclinic orbits for the fixed points  $T_{\pm}$ ,

$$H0 : \quad T_+ \rightarrow T_+ \quad \text{and} \quad T_- \rightarrow T_- ,$$

the heteroclinic orbits joining  $D_-$  to  $D_+$  in the  $r \equiv 0$  plane,

$$H1 : \quad D_- \rightarrow D_+ ,$$

the heteroclinic orbit joining  $D_+$  to  $D_-$  which leaves the  $r \equiv 0$  plane at these critical points,

$$H2 : \quad D_+ \rightarrow D_- ,$$

the heteroclinic orbits joining  $T_+$  and  $T_-$ ,

$$H3 : \quad T_- \rightarrow T_+ \quad \text{and} \quad T_+ \rightarrow T_- ,$$

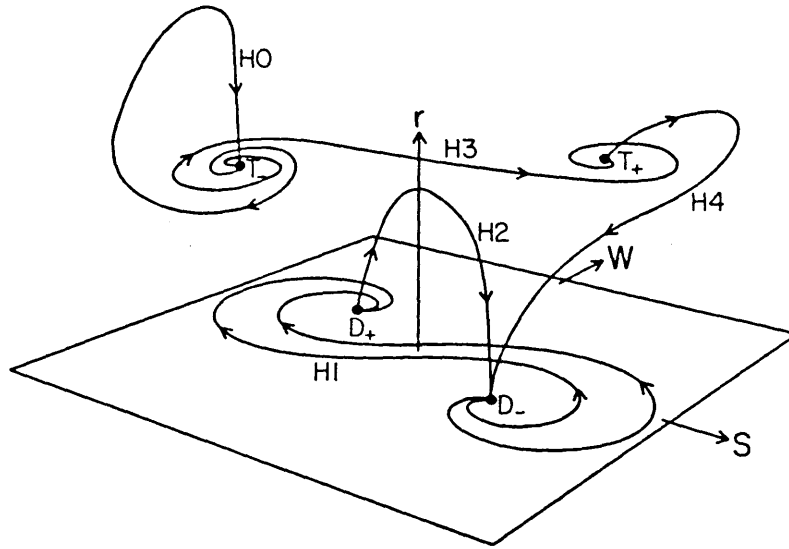


Figure 4.5: Orbits in the 3D system as examples of homoclinic ( $H0$ ) and heteroclinic connections ( $H1 - H4$ ).

and the orbits joining  $D_{\pm}$  and  $T_{\pm}$ ,

$$H4: \quad D_+ \rightarrow T_{\pm} \quad \text{and} \quad T_{\pm} \rightarrow D_- .$$

These orbits are illustrated in Figure 4.5 although it should be understood that not all of these orbits exist simultaneously for given values of  $\Omega$  and  $c$ .

The orbits  $H4$  describe the transition from undisturbed Poiseuille flow to finite amplitude waves and are structurally stable in the sense that they persist under perturbations in both  $\Omega$  and  $c$ . Numerical computations suggest that the  $H4$  orbits ( $T_+ \rightarrow D_+$ ) exist in the entire region IVa of parameter space for compliant as well as rigid walls. Figure 4.6 is a typical example of  $H4$  for both rigid walls and  $\kappa = 1.1 \times 10^7$  where  $\Omega = 10.0$  and  $c = 20.0$ .

The orbits  $H3$  are transitions between finite amplitude waves of different amplitudes and would be expected to exist throughout regions IIa and IIb. Figure 4.7 is an example of  $H3$  for rigid and compliant walls where  $\Omega = 10.0$  and  $c = 9.0$ . This

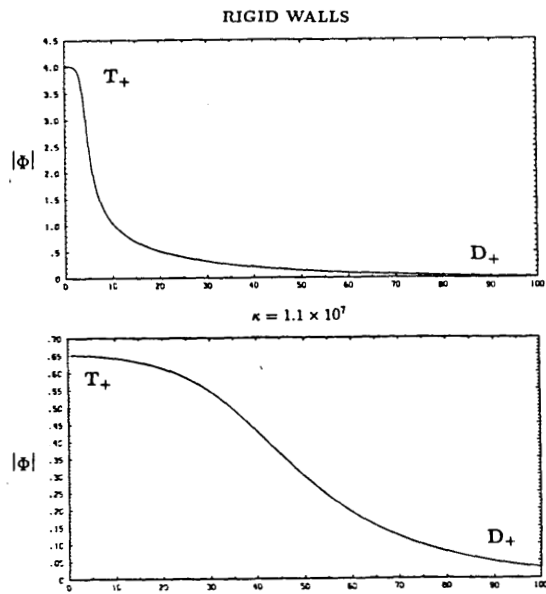


Figure 4.6: The heteroclinic connection  $H4$  from a plane wave to a zero amplitude solution at  $\Omega = 10$  and  $c = 20$  .

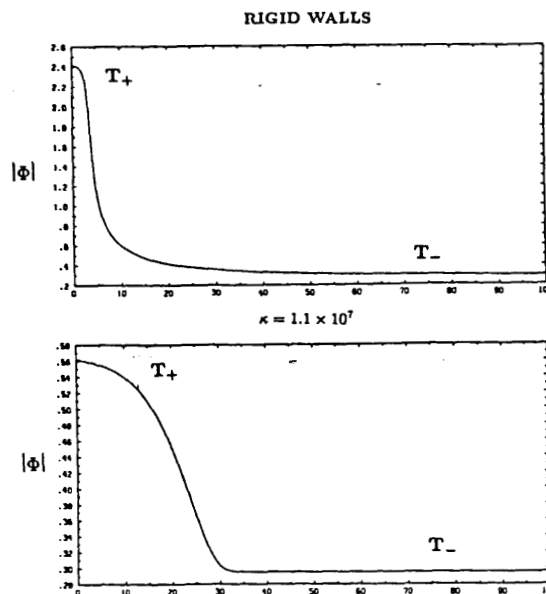


Figure 4.7: The heteroclinic connection  $H3$  between two plane waves with different amplitudes at  $\Omega = 10$  and  $c = 9$  .

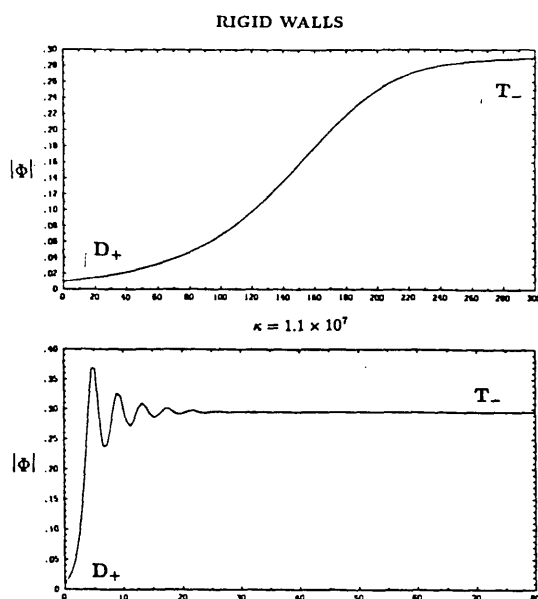


Figure 4.8: The heteroclinic connection  $H4$  from a zero amplitude solution to a plane wave at  $\Omega = 10$  and  $c = 9$  .

same point in parameter space also has as  $H4$  orbit from  $D_+ \rightarrow T_-$  (Figure 4.8).

In Figure 4.9 an orbit in  $(r, s, w)$  space is shown for  $\Omega = 20.0$  and  $c = 0.96$  , and Figure 4.10 is the orbit for  $\kappa = 1.1 \times 10^7$  for the same parameter values ( $r$  is in the  $z$ -direction in these plots). When  $\Omega = 10.0$  the critical point  $T_-$  undergoes a Hopf bifurcation at  $c = 1.726$  and  $c = 3.599$  for rigid and compliant boundaries, respectively, and the periodic orbit undergoes a period doubling bifurcation at  $c = 1.210$  for rigid walls and remains stable to  $c = 0$  for compliant walls. The orbit for rigid walls (Figure 4.9) appears to approach a nonperiodic and possibly chaotic attracting set, and the orbit for  $\kappa = 1.1 \times 10^7$  approaches (very slowly) a stable periodic orbit. I have been unable to find any period doubling bifurcations for  $\kappa = 1.1 \times 10^7$  or orbits like that in Figure 4.9, and from this evidence I claim that the “chaotic” solutions found when  $d_r = +1$  do not exist when  $d_r = -1$  .

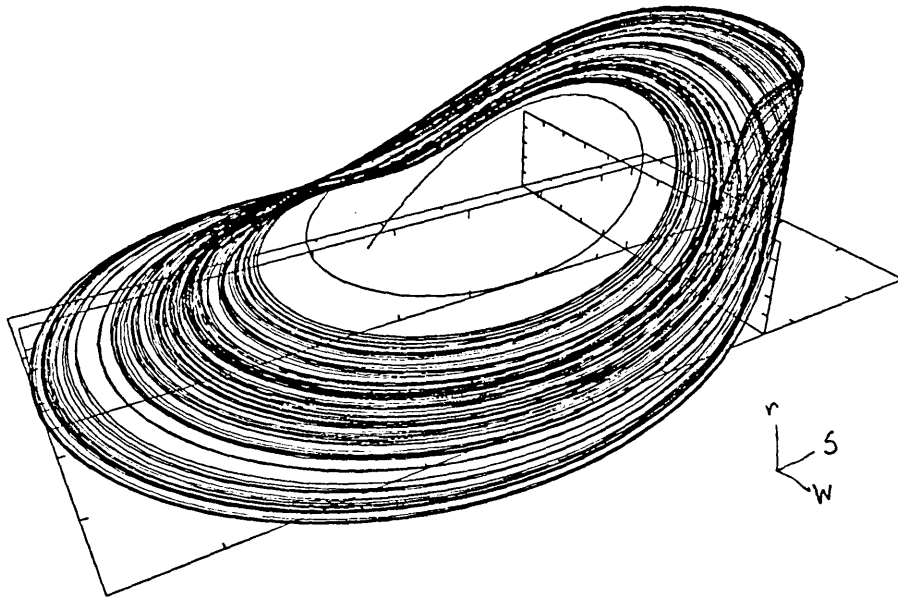


Figure 4.9: A nonperiodic orbit at  $\Omega = 10$  and  $c = 0.96$  for rigid wall boundary conditions.

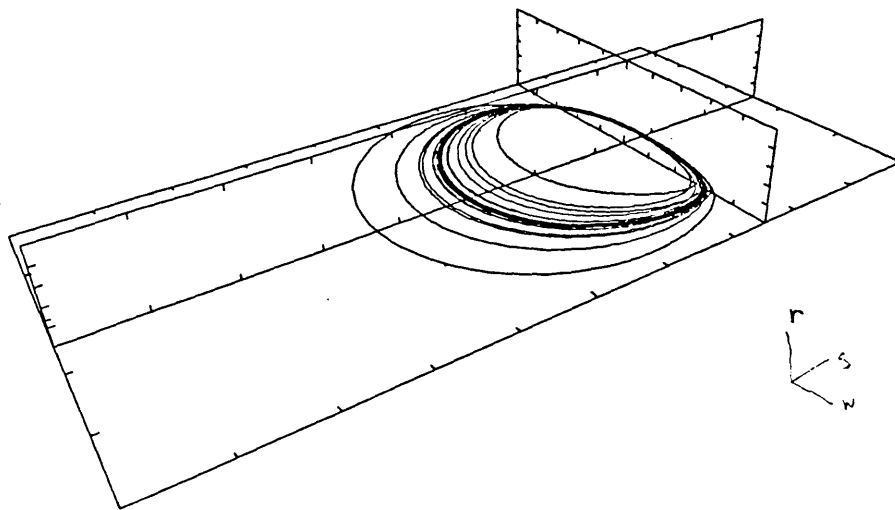


Figure 4.10: An attracting periodic orbit at  $\Omega = 10$  and  $c = 0.96$  for compliant wall boundary conditions ( $\kappa = 1.1 \times 10^7$ ).

# Chapter 5

## Conclusions

The two-dimensional finite amplitude traveling wave solutions which bifurcate from the Orr-Sommerfeld curve for the linear stability of Poiseuille flow are of the form

$$\Psi = F(x - c_p t, y, Re, \alpha)$$

where  $F$  is of period  $2\pi/\alpha$  in the first variable and  $c_p$  is determined by  $\alpha$  and  $Re$ . These equilibrium states are found on a surface in  $Re$ ,  $\alpha$ , amplitude space illustrated for rigid boundaries in Figure 5.1 (J.P.Zahn, *et al.*, [1974]; Herbert, [1981]; Landman, [1987]). For  $Re < Re_c$  the zero amplitude solutions are stable equilibria and the lower branch of the finite amplitude surface is unstable. Although the calculation of this nonlinear neutral surface for compliant boundaries is beyond the scope of this thesis, the weakly nonlinear calculations show that for small amplitude near  $Re = Re_c$  and  $\alpha = \alpha_c$  the finite amplitude solutions are stable for  $Re > Re_c$ . I have shown by direct calculation that values of the compliancy parameters  $B$ ,  $T$ ,  $\kappa$ ,  $M$ , and  $d$  exist where  $d_r = -1$ , and, consequently, the bifurcation to finite amplitude solutions must be supercritical at  $Re = Re_c$  and  $\alpha = \alpha_c$ .

These results may also be true for other flows where there is a neutral curve of the Orr-Sommerfeld type, in particular boundary layer flow. In the Blasius boundary layer the Reynolds number (based on the displacement thickness) grows like the square root of the distance from the leading edge, and, consequently, at some point on the plate the flow reaches  $Re_c$  and begins to grow exponentially. These growing solutions are generally believed to be unstable to three-dimensional disturbances (Squire's theorem only concerns the initial, linear disturbance), and experiments show that three-dimensional perturbations grow rapidly once the Tollmien-Schlichting waves

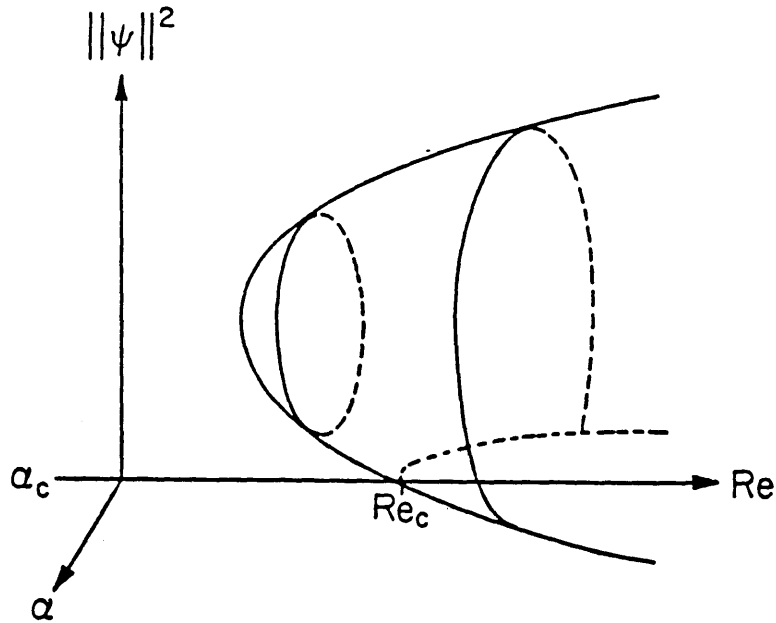


Figure 5.1: Surface of two-dimensional finite amplitude traveling waves for rigid wall Poiseuille flow as a function of Reynolds number and wavenumber.

reach a threshold amplitude of about 1% of the free stream velocity (Bayly, *et al.*, [1988]). If, however, the compliancy parameters are such that the bifurcation is supercritical, then the growth of the amplitude is initially linear (along the nonlinear neutral curve), and the transition to large amplitude three-dimensional disturbances is delayed. Further analysis of this bifurcation using a time dependent Navier-Stokes calculation would be illuminating.

There is little evidence I am aware of that supports the idea that fully developed turbulence can be modeled by an attracting set of small dimension imbedded in the very large dimensional state space of the fluid system. Nevertheless, a recent experimental study of Rayleigh-Bénard convection (B. Castaing, G. Gunaratne, F. Heslot, L. Kadanoff, A. Libchaber, S. Thomae, X.-Z. Wu, S. Zaleski, G. Zanetti, [1988]) shows that while most of the previous investigators describe the fluid as turbulent as

soon as the behavior is nonperiodic, there is actually a nonperiodic behavior which is very different from fully developed turbulence. In this nonperiodic state (which the authors call “chaotic”) only the time coherence is lost while the space coherence persists. This result should be compared to the nonperiodic envelope solution in the slow variable  $X = x - c\tau$  shown in Figure 4.9. If this nonperiodic solution of the Ginzburg-Landau equation corresponds to a set of chaotic intermediate states between laminar flow and turbulence, then its absence when  $d_r = -1$  indicates that the process by which turbulent flow develops and replaces laminar flow has changed in a fundamental way. Whether it changed to such an extent to explain Kramer’s experimental results is still an open question.

# Appendix A

## Orr-Sommerfeld maximum growth rate

The Orr-Sommerfeld neutral stability curve illustrated in Figure 1.1 divides the  $\alpha$ -Reynolds number plane into a region where  $c_i$  is less than zero and one where  $c_i$  is greater than zero. Shen [1954] calculated curves of constant  $c_i$  by perturbing the neutral curve obtained by Lin [1945] for plane Poiseuille flow and found that  $c_i$  reached a maximum of 0.0076 at  $\alpha = 0.79$  and  $Re = 48000$ . If there exists a more recent calculation of the maximum value of  $c_i$ , denoted here as  $c_{imax}$ , then it is not widely known since both Orszag and Patera [1983] and Bayly, *et al.* [1988] cite these results (although there is no specific reference to Shen). I have found that the value of  $c_{imax}$  is 0.01051 at  $Re = 105029$  and  $\alpha = 0.674$ .

This value of  $c_{imax}$  was found using multiparameter continuation. First I fixed the value of the Reynolds number and increased  $c_i$  (leaving  $\alpha$  free to vary) until  $c_i$  reached a maximum (a fold in  $\alpha - c_i$  space). Then I increased  $c_i$  again allowing both the Reynolds number and  $\alpha$  to vary in a two parameter continuation described in Keller [1987] and implemented in the AUTO program (Doedel and Kernevez, [1985]). Table 6 shows the values of  $\alpha$ ,  $Re$ , and  $c$  at this fold point when 101 and 141 grid points are used to solve the Orr-Sommerfeld equation. This type of fold point is called an elliptic point. Figure A1 illustrates the location of this point within the contour  $c_i = 0.0104$  in the  $\alpha$ -Reynolds number plane (The curve  $c_i = 0$  cannot be seen on this scale).

The discrepancy between this result and Shen's calculation is due to his method of calculation. He calculated the rate of change for  $c$  in both the  $\alpha$  and  $Re$  direction at points along the neutral stability curve obtained by Lin, fit these rates to a cubic

|          | 101 grid points | 141 grid points |
|----------|-----------------|-----------------|
| $\alpha$ | 0.6740137       | 0.6740131       |
| $Re$     | 105028.8        | 105029.4        |
| $c_r$    | 0.1279359       | 0.1279357       |
| $c_i$    | 0.01051284      | 0.0151284       |

Table A.1: The location of the maximum value of  $c_i$  in the  $\alpha - Re$  plane.

in  $\alpha$  at constant  $Re$ , and interpolated to find the contours of constant  $c_i$ . The critical Reynolds number found by Lin's procedure is about 10% too low, and Shen points out that the errors he introduces by interpolation could be as large as 20%. Along with those introduced by the polynomial approximation, these errors account for the difference between Shen's result and my numerical one.

This value of  $c_{imax}$  does not alter conclusions based on the old value. Bayly, *et al.*, [1988] note that at a Reynolds number of 48,000 the growth rate of the periodic disturbance is a factor of 10 in 300 non-dimensional time units, and, compared to the explosive growth observed experimentally over a few channel widths, the instability is quite feeble. For the actual maximal growth rate attained at  $Re = 105029$ , a factor of 10 is attained in 220 non-dimensional time units. The conclusion that the growth rates induced by viscosity are small compared to the convective timescale is still a valid one.

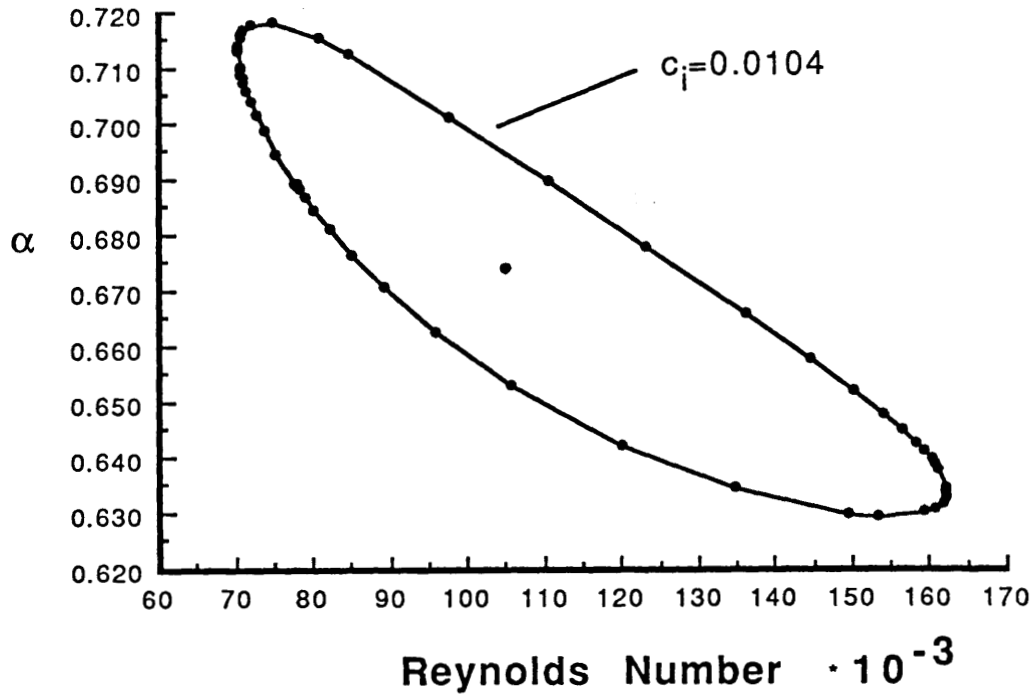


Figure A.1: Contour of  $c_i$  in the  $\alpha - Re$  plane.

# Appendix B

## The calculation of $c_g$

In this appendix I will describe the method I used to calculate the value of  $c_g$  numerically. The method should be applicable to any inhomogeneous boundary value problem with an undetermined constant on the right-hand side. Let me begin with a simple example.

The requirement for the existence of a solution to the boundary value problem

$$\frac{d^2w}{dx^2} + w = \sin x - d \quad w(0) = 0, \quad w(\pi) = 0, \quad (\text{B.1})$$

to exist is a solvability condition:

$$\int_0^\pi \sin x (\sin x - d) dx = 0 \quad \rightarrow \quad d = \pi/4. \quad (\text{B.2})$$

If  $d$  is not equal to  $\pi/4$  there is no solution to equation B.1, and if  $d$  is equal to  $\pi/4$  the solution is

$$w(x) = C \sin x - \frac{x \cos x}{2} + \frac{\pi}{4}(\cos x - 1).$$

where  $C$  is an arbitrary constant. This arbitrary constant can be fixed by an additional boundary condition independent of those in equation B.1:

$$w'(0) = 0 \quad \rightarrow \quad C = 1/2.$$

This integration method (equation B.2) is used by Stewartson and Stuart [1971] to calculate  $c_g$  (where  $c_g$  corresponds to  $d$  in equations B.1 and B.2).

The program AUTO developed by Doedel and Kernevez [1985] calculates solution branches of systems of ODEs by a collocation method on an adaptive mesh. I solve equation 3.2 with AUTO by letting  $c_g$  be an unknown parameter and adding the

independent boundary condition

$$\psi_{10}(0) = 0$$

to the flexible boundary conditions (equations 3.7) for  $\psi_{10}$  . When this system (equation 3.2 and the boundary conditions) is solved numerically, not only is a value for  $c_g$  found which agrees with the previous (rigid wall) results, but the value of the imaginary part of  $c_g$  (which should be zero) is much smaller than that found using integration (the solvability condition). I interpret this result to mean that integration gives a less accurate numerical result than the alternative method described here.

Since the integration of the right-hand side of equation 3.2 multiplied by the adjoint function does not require the calculation of  $\psi_{10}$  it is the less computationally expensive method to find  $c_g$  , but because I need calculate  $\psi_{10}$  to obtain the higher order Ginzburg-Landau coefficients, I effectively get  $c_g$  at no cost at all. All of the other Ginzburg-Landau coefficients are found using integration.

## Bibliography

- Bayly, B.J., Orszag, S.A., Herbert, T. [1988] Instability mechanisms in shear-flow transition. *Ann. Rev. Fluid Mech.* **20**, 487-526.
- Benjamin, T.B. [1960] Effects of a flexible boundary on hydrodynamic stability. *J. Fluid Mech.* **9**, 513-532.
- Benjamin, T.B. [1964] Fluid flow with flexible boundaries. *Proc. 11th Intl. Congr. Appl. Maths Munich, Germany* (ed. H. Görtler) 109-128, Springer-Verlag.
- Blennerhassett, P.J. [1980] On the generation of waves by wind. *Phil. Tran. Roy Soc. Lon.* **298**, 451-494.
- Carpenter, P.W., Garrad, A.D. [1985] The hydrodynamic stability of flow over Kramer-type compliant surfaces. Part 1. Tollmien-Schlichting instabilities. *J. Fluid Mech.* **155**, 465-510.
- Carpenter, P.W., Garrad, A.D. [1986] The hydrodynamic stability of flow over Kramer-type compliant surfaces. Part 2. Flow-induced surface instabilities. *J. Fluid Mech.* **170**, 199-232.
- Castaing, B., Gunaratne, G., Heslot, F., Kadanoff, L., Libchaber, A., Thomae, S., Wu, X.Z., Zaleski, S., Zanetti, G. [1988] Scaling of hard thermal turbulence in Rayleigh Benard convection. preprint.
- Davey, A., Hocking, L.M., Stewartson, K. [1974] On the nonlinear evolution of three-dimensional disturbances in plane Poiseuille flow. *J. Fluid Mech.* **63**, 529-536.

- Doedel, E.J., Kernevez, J.D. [1985] Software for continuation and bifurcation problems. *Applied Math. Tech. Rep.*, Caltech.
- Drazin, P.G., Reid, W.H. [1981] *Hydrodynamical Stability*. Cambridge University Press.
- Gray, J. [1957] How fishes swim. *Sci. Am.* **197**, # 2, 48-54.
- Guckenheimer, J., Holmes, P. [1983] *Nonlinear oscillations, dynamical systems, and bifurcations of vector fields*. Springer-Verlag.
- Gwan, R.W.L. [1948] Aspects of the locomotion of whales. *Nature* **161**, 44-46.
- Hains, F.D., Price, J.F. [1962] Effect of a flexible wall on the stability of Poiseuille flow. *Phys. Fluids* **5**, 365.
- Herbert, T. [1981] A secondary instability mechanism in plane Poiseuille flow. *Bull. Am. Phy. Soc.* **26**, 1257.
- Keller, H.B., [1987] *Numerical methods in bifurcation problems*. Springer-Verlag.
- Korotkin, A.I. [1965] The stability of a laminar boundary layer on an elastic surface in an incompressible fluid. (in Russian) *Izv. Akad. Nauk SSSR, Mekh. Zhid. i Gaza* no. 3, 39-44.
- Kramer, M.O. [1961] The dolphins' secret. *J. of the American Society of Naval Engineers* **73**, 103-107.
- Kramer, M.O. [1965] Hydrodynamics of the dolphin. *Adv. in Hydroscience* **2**, 111-130.
- Landahl, M.T. [1962] On the stability of a laminar incompressible boundary layer over a flexible surface. *J. Fluid Mech.* **13**, 609-632.
- Landahl, M.T., Kaplan, R.E. [1965] Effect of compliant walls on boundary layer stability and transition. *AGARDograph* 97-1-353.

- Landman, M.J. [1987] Solutions of the Ginzburg-Landau equation of interest in shear flow transition. *Studies in Applied Math.* **76**, 187-237.
- Lin, C.C. [1945] On the stability of two-dimensional parallel flows. *Quart. Appl. Math.* **3**, 117-142.
- Orszag, S.A., Patera, A.T. [1983] Secondary instability of wall-bounded shear flows. *J. Fluid Mech.* **128**, 347-385.
- Riley, J.J., Gad-el-Hak, M., Metcalfe, R.W. [1988] Compliant coatings. *Ann. Rev. Fluid Mech.* **20**, 393-420.
- Shen, S.F. [1954] Calculated amplified oscillations in the plane Poiseuille and Blasius flows. *J. Aero. Sci.* **21**, 835-48.
- Sirovich, L., Newton, P.K. [1986] Periodic solutions of the Ginzburg-Landau equation. *Physica* **21D**, 115-125.
- Squire, H.B. [1933] On the stability of three-dimensional disturbances of viscous flow between parallel walls. *Proc. Roy. Soc. A* **142**, 621-628.
- Stewartson, K., Stuart, J.T. [1971] A non-linear instability theory for a wave system in plane Poiseuille flow. *J. Fluid Mech.* **48**, 529-545.
- Zahn, J.P., Toomre, J., Spiegel, E.A., Gough, D.O. [1974] Nonlinear cellular motions in Poiseuille channel flow. *J. Fluid Mech.* **64**, 319-345.